# RF RECEIVER SYSTEMS FOR W-CDMA TECHNOLOGY

Estela Romero Muñoz
Tampere Polytechnic
June of 2005

# INDEX

# *PART I*

# *W-CDMA FOR UMTS*

# CHAPTER I

# INTRODUCTION TO W-CDMA

## 1.1 W-CDMA IN THIRD GENERATION SYSTEMS

The evolution of mobile telecommunication services can be easily identified by the different mobile communication system generations. First generation systems consisted of analog networks offering solely speech oriented services. Second generation digital systems had the aim to develop a global system and pretended to offer supplementary services and several data oriented services in addition to the existing speech oriented services. The second generation has widely reached its purposes specially the European solution: GSM. An intermediate solution, known as 2.5 generation, was adopted in order to offer new data oriented services, due to the difficulties in the third generation launching.

The purpose of the third generation was to offer a global standard. In order to attain this aim, the *International Telecommunication Union* (ITU) defined the *International Mobile Telecommunication 2000* (IMT-2000). The main aims of this standard are:

- Full coverage and mobility at 144 and 384 Kbps bit rates.
- Limited coverage and mobility with bit rates down to 2 Mbps.
- High spectral efficiency compared to existing systems.
- Flexibility to introduce new services.
- Possible use of a satellite component, in addition to the terrestrial component.

In order to settle a global compatibility, the *World Administrative Radio Conference* (WARC) of the ITU, at its 1992 meeting, defined the operating frequency bands for third generation systems. Specifically, the bands comprised among 1885-2025 MHz and 2110-2200 MHz were assigned for third generation

systems. Assigned bands and spectrum allocation for the different regions can be observed in **figure 1.1**.

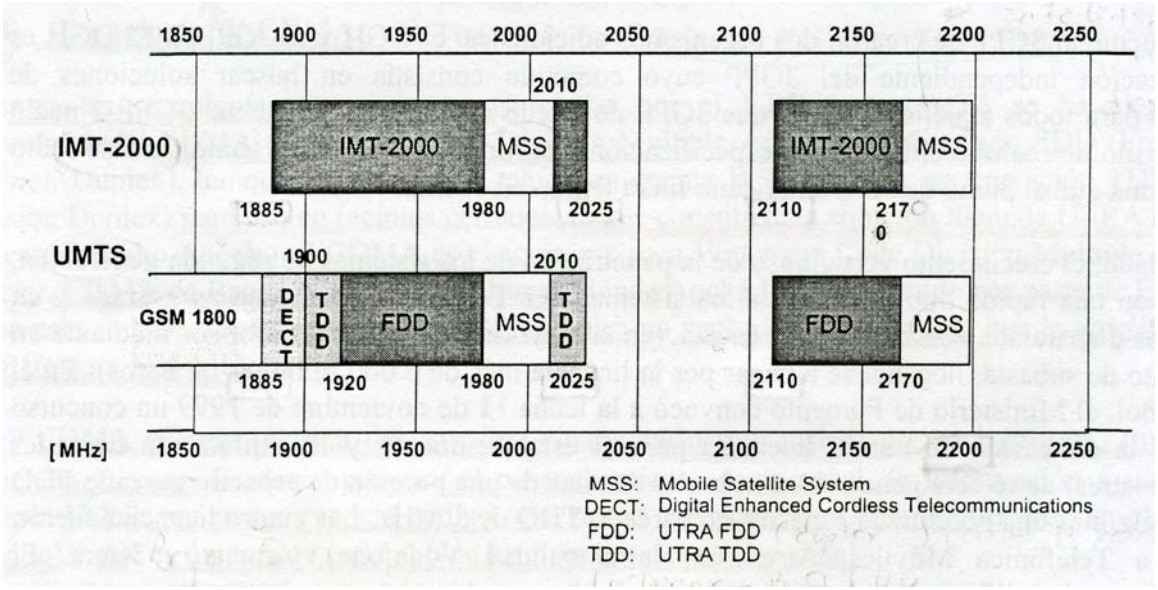


**Figure 1.1** Frequency allocations for IMT-2000 and UMTS

However, due to the different proposals from the regional organizations, a global third generation system has been impossible to adopt. There are five different proposals for the air interface, grouped in four families, as can be seen in **table 1.1**.

| Name | Proposal | Access Technology |
|---|---|---|
| IMT-DS Direct Spread | UTRA | CDMA |
| IMT-TC Time Code | UTRA | CDMA/TDMA |
| IMT-MC Multi Carrier | MC CDMA 2000 | CDMA |
| IMT-SC Single Carrier | UWC-136 | TDMA |
| IMT-FT Frequency Time | DECT | TDMA/FDMA |

**Table 1.1** IMT-2000 terrestrial component interfaces

Thus IMT-2000 consists of a family of systems, highly compatible each others, ensuring at least worldwide roaming by using of multimode terminals.

The proposal coming from the *European Telecommunication Standard Institute* (ETSI) as third generation system for Europe was named as *Universal Mobile Telecommunication System* (UMTS). UMTS includes two methods for the *UMTS Terrestrial Radio Access* (UTRA), *Frequency Division Multiple Access* (FDD) and *Time Division Multiple Access* (TDD) due to the impossibility to find a common agreement. The frequency allocations for these two methods are shown in **table 1.2**.

| | Uplink | | Downlink | Total |
|---|---|---|---|---|
| UMTS-FDD | 1920-1980 | | 2110-2170 | 2x60 MHz |
| UMTS-TDD | 1900-1920 | and | 2010-2025 | 20+15 MHz |

**Table 1.2** Frequency allocations for FDD and TDD modes

In FDD mode, separate 5 MHz carrier frequencies are used for the uplink and downlink respectively, whereas in TDD mode only one 5 MHz carrier is time-shared between uplink and downlink.

In order to develop a global system, a forum was created. This forum, called *Third Generation Partnership Project* (3GPP) specifies the system in a more global way. The 3GPP forum is made up for organizations from Europe, Japan, Korea, China and E.E.U.U.

### 1.1.1 GENERAL UMTS SYSTEM CHARACTERISTICS

UMTS will be a mobile telecommunication system able to offer significant profits to the users including high quality and wireless multimedia services through a convergent network. UMTS will provide information and new services and applications directly to the users.

One fundamental aim of UMTS system is to offer a wide variety of voice, data and multimedia services under an extremely competitive and dynamic environment. The main features of UMTS are:

- Synchronous and asynchronous transmission capacity.
- 384 Kbps bit rates and up to 2 Mbps under low mobility conditions.
- Data transmission support in circuit-switched mode and packet-switched mode.
- Higher capacity and efficient spectrum use than the existing systems.
- High quality and security level.
- Support of simultaneous services by means of Bandwidth on Demand (BoD) assignment.
- International roaming among IMT-2000 operators.

- Coexistence and interconnection with satellites.

## 1.2 MAIN PARAMETERS IN W-CDMA

Among all access technologies considered by the standardization forums, W-CDMA has been the most widely adopted third generation air interface. W-CDMA is the acronym for *Wideband Code Division Multiple Access*. The term *wideband* was incorporated for Europe and Japan to point to their CDMA version employs a wider bandwidth than the American version (5 MHz instead of 1.25 MHz).

W-CDMA is a DS-CDMA system. The user information bits are spread over a wide bandwidth by multiplying the user data with a spreading code. This code sequence is unique for all the users belonging to a same channel. In the UMTS system the spreading code chip rate is constant and equal to 3.84 Mcps. The channel bandwidth is 5 MHz including guard bands.

Advantages of DS-CDMA:

- Multiple access capacity
- Protection against multipath interference
- Security: the transmitted signal can be recovered only if its spreading sequence is known
- Immunity against the interference
- Coherent demodulation of the wideband desired signal is possible
- Synchronization among users is not necessary

W-CDMA supports variable user data rates. Each user is allocated in frames of 10 ms duration, during which the user data rate is kept constant. However, the

data capacity among the users can change from frame to frame. The 10ms W-CDMA frame is divided in 15 slots, 2/3 ms duration each one. As W-CDMA chip rate is 3.84 Mcps, chip duration is 0.26041 μs. Thus, chips number per slot is 2560 and there are 38400 chips per frame.

**Table 1.3** summarizes the main parameters and physical layer characteristics related to W-CDMA air interface.

| | |
|---|---|
| **Radio access technique** | DS-CDMA |
| **Chip rate/ Bandwidth** | 3.84Mcps/ 5MHz |
| **Frame length** | 10 ms |
| **Duplexing method** | FDD/ TDD |
| **Modulation** | BPSK in uplink/ QPSK in downlink |
| **Codification** | Convolutional or turbo code |
| **Base station synchronization** | Asynchronous operation |
| **Multirate concept** | Variable spreading factor and multicode |
| **Service multiplexing** | Multiple services with different quality of service requirements multiplexed on one connection |
| **Detection** | Coherent |
| **Power control** | Open-loop, inner and outer closed-loop |
| **Diversity** | By Rake receptor, antenna diversity and transmit diversity |
| **Handovers** | Inter-mode, intra-mode and inter-system. Hard, soft and softer. |

**Table 1.3** W-CDMA main parameters and physical layer characteristics

## 1.2.1 W-CDMA SIGNAL GENERATION

The process of a W-CDMA signal generation is implemented in two steps, as can be seen in **figure 1.2**. The first step consists of multiplying our desired data sequence by a spreading or channelization code in order to widen the user signal's spectrum to transmit. The spreading factor, SF, will be chosen depending on the user data signal bit rate, so that the result of multiply SF by user data signal bit rate keeps constant and equal to 3.84Mcps. Spreading codes identify all the users belonging to a same cell, so aforementioned codes have to be orthogonal each others in order to minimize the interference among users.

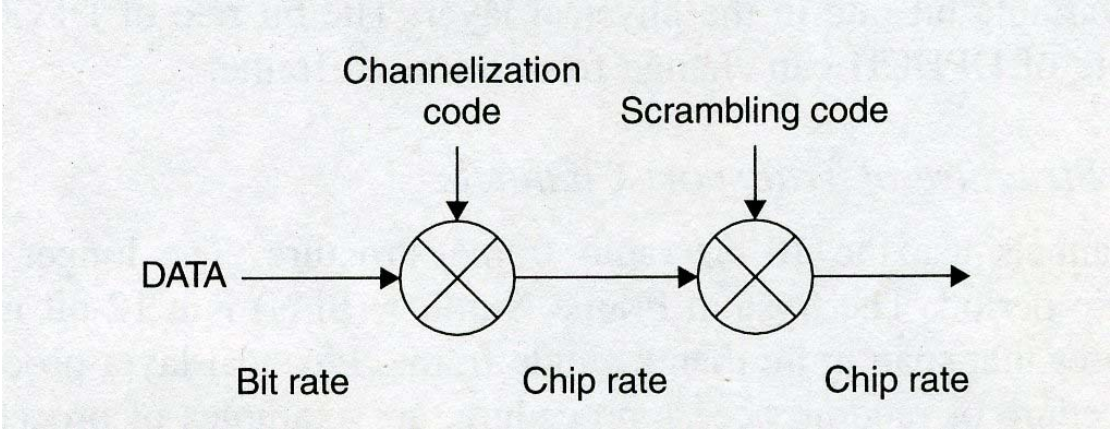


**Figure 1.2** W-CDMA signal generation

In the second step, the sequence before generated is multiplied by a scrambling code. This multiplication is made in order to separate communications from the different cells. Thereby, a same spreading code can be used for several cells simultaneously. Thanks to the utilization of two code families, the number of users our system can offer services to will be increase.

## 1.2.2 COMPARISON BETWEEN W-CDMA AND SECOND GENERATION AIR INTERFACES

In this section, differences between W-CDMA and the second generation standards GSM and IS-95 (standard for cdmaOne) are considered.

Second generation systems were built in order to provide voice services. Third generation systems have to fulfill new requirements such as bit rates up to 2 Mbps, bandwidth on demand support, coexistence with second generation systems and high spectrum efficiency. Therefore, W-CDMA air interface must have the proper characteristics to fulfill the requirements.

A comparison between these three standards is shown in **table 1.4**. The differences in the air interface show the new W-CDMA requirements. 5 MHz bandwidth is needed to support high bit rates and transmit diversity to support asymmetric capacity in downlink. Advanced radio resource management algorithms are needed to guarantee quality of service and maximize system throughput. The high chip rate of 3.84Mcps provides higher multipath diversity which improves the coverage. W-CDMA is designed to operate with asynchronous base stations so synchronization from GPS is not required. Is-95 needs GPS because its base stations have to be synchronized.

| | W-CDMA | GSM | IS-95 |
|---|---|---|---|
| **Carrier spacing** | 5 MHz | 200 KHz | 1.25 MHz |
| **Frequency reuse factor** | 1 | 1-18 | |
| **Chip rate** | 3.84Mcps | | 1.2288Mcps |
| **Power control frequency** | 1500 Hz, both uplink and downlink | 2 Hz or lower | 800 Hz en uplink, downlink: slow power control |
| **Quality control** | Radio resource management algorithms | Network planning (Frequency planning) | |
| **Frequency diversity** | Rake receptor | Frequency hopping | Rake receptor |
| **Base station synchronization** | Not needed | | Typically obtained via GPS |
| **Efficient radio resource management algorithms** | Yes, provides required quality of service | | Not needed for speech only networks |
| **Packet data** | Load-based packet scheduling | Time slot based scheduling with GPRS | Packet data transmitted as short circuit switched calls |
| **Intra-system handover** | Soft/softer handover | Hard handover | Soft/softer handover |
| **Inter-system handover** | GSM handover | | AMPS handover |
| **Transmit diversity** | Supported in downlink | No supported | Supported in downlink |

**Table 1.4** Differences between W-CDMA and second generation air interfaces

## 1.3 RADIO ACCESS NETWORK SYSTEM ARCHITECTURE

The UMTS system consists of a number of logical network elements that each has a defined functionality. These network elements can be grouped based on similar functionality. Under this point of view, the network elements are grouped in:

- Core Network (CN), responsible of call commutation and routing and data connections to external networks.

- UMTS Terrestrial Radio Access Network (UTRAN) which manages the radio functionality.
- User Equipment (UE): mobile terminals enabling the interface between user and radio network.

Under the standardization and specifications point of view, UE and UTRAN adopt new protocols which design is based on new W-CDMA technology requirements. On the other hand, CN adopt the first version corresponding to GSM/GPRS.

Another way to group UMTS network elements is to divide them into several sub-networks. The UMTS system is modular because it is possible to have several network elements of the same type. Having several entities of the same type allows the division of the UMTS system into sub-networks that are operational either on their own or together with other sub-networks, and that are distinguished from each other with unique identities. Such a sub-network is called a UMTS PLMN (Public Land Mobile Network). Typically one PLMN is operated by a single operator, and is connected to other PLMNs as well as to other types of networks, such as ISDN, PSTN, the Internet, and son on. **Figure 1.3** shows elements in a PLMN and the connections to external networks.

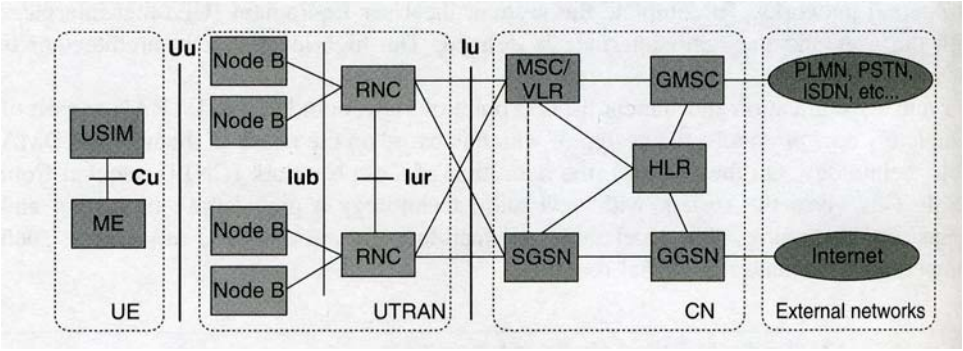


**Figure 1.3** Network elements in a PLMN

The UE consists of two parts:

- The Mobile Equipment (ME), radio terminal used for radio communication over the Uu interface.
- UMTS Subscriber Identity Module (USIM), smart card that holds the subscriber identity, performs authentication algorithms and stores authentication and encryption keys and some subscription information needed in the terminal.

The main propose of the UTRAN is to establish a communication link between the UE and the CN by means of the radio access bearer (RAB) service, with a quality of service requirements defined by the CN. The UTRAN consists of Radio Network Systems (RNS) connected to the CN over the Iu interface. A RNS consists of one Radio Network Controller (RNC) element and one or more Node B entities connected to the RNC over the Iub interface.

- The RNC manages the radio resources in its domain (the node B's connected to it) over the Iub interface. Several RNCs can also be interconnected each others over the Iur interface.
- The node B or Base Station manages a group of cells converting the data flow between the RNC over the Iub interface and the UE over the Uu interface. It also participates in the radio resource management.

This architecture permit an in-scale RNS dimensioning and a considerable mobility management capacity. Both the node B and the RNC are able to manage handovers and macrodiversity maintaining the current connection between the mobile terminal and the network using more than one base station. This property is quite important in CDMA systems.

The CN is the basic platform for all the communication services that are provided for UMTS subscribers, including both telephony and packet-data services. The main elements in the CN are the same than in GSM/GPRS networks.

- The Home Location Register (HLR) is a database located in the user's home system that stores the master copy of the user's service profile. The service profile consists of, for example, information on allowed services, forbidden roaming areas, and Supplementary Service information such a status of call forwarding and the call forwarding number. It is created when a new user subscribes to the system, and remains stored as long as the subscription is active.
- The Mobile Services Switching Centre/Visitor Location Register (MSC/VLR) is the switch and the database that serves the UE in its current location for Circuit Switched (CS) services. The MSC function is used to switch the CS transactions, and the VLR function holds a copy of the visiting user's service profile, as well as more precise information on the UE's location within the serving system. The part of the network that is accessed via the MSC/VLR is often referred to as the CS domain.
- The Gateway MSC (GMSC) is the switch at the point where UMTS PLMN is connected to external CS networks. All incoming and outgoing connections go through GMSC
- The Serving GPRS Support Node (SGSN) has the same functionality as MSC/VLR but is typically used for Packet Switched (PS) services. The part of the network that is accessed via the SGSN is often referred to as the PS domain.
- The Gateway GPRS Support Node (GGSN) has a similar functionality than GMSC but is related to PS services.

The external networks are divided in two groups: CS networks like ISDN and PSTN networks providing circuit-switched connections, for example the existing telephony service and PS networks like the Internet providing connections for packet data services.

The UMTS standards have been structured in such a way that network elements internal functionality is not specified in detail. However, the interfaces among logical elements have been well-defined. The following open interfaces have been specified:

- The Cu interface is the electrical interface between the USIM smart card and the ME. The interface employs a standard format for all the cards.
- The Uu interface is the W-CDMA radio interface. The UE access to the fixed part of the system over this interface. It is probably the most important interface in UMTS.
- The Iu interface connects the UTRAN to the CN.
- The Iur interface connects RNCs each others and permits soft handovers between RNCs from different manufacturers.
- The Iub interface connects one Node B to a RNC.

# CHAPTER II

# RADIO NETWORK PLANNING

The W-CDMA radio network planning process consists of three parts: dimensioning, capacity and coverage planning and network optimization.

This planning process treats to estimate the numbers of base station sites and their configurations, to calculate parameters of network elements and to analyze network capacity, coverage and quality of service conditions.

# 2.1 DIMENSIONING

In the dimensioning phase, network configurations and amount of network elements are estimated basing on operator's requirements for coverage, capacity and quality of service.

## 2.1.1 RADIO LINK BUDGETS

In this section the radio link budget in uplink direction will be calculated as uplink interference (noise from other mobiles) is usually the limiting factor in CDMA systems.

In the radio link budget calculation, W-CDMA specific parameters are taken in account. These parameters are interference margin, fast fading margin and soft handover gain.

The steps to follow in uplink budget calculation are:

**1._** To define the required data rate/s for each network area and $Eb/N_0$ targets. These are usually defined by the operator, but simulation tools can be used to

tailor the $Eb/N_0$. Simulation can be done by creating an uniform base station and a mobile distribution plan with defined service profiles.

**2._** To gather vendor's specific data as base station output power and receiver noise figure, defined and used cable systems, possible additional lineal amplifiers, used diversities (antenna, polarization, receiver),etc.

**3._** The network operator has to define, for each geographic areas, $Eb/N_0$, data services, system loading factor, estimated mobile speeds, different penetration losses, coverage reliability and used fade margin.

**4._** Mobile power levels, bit rate and processing gains are defined for all UMTS standards. Soft handover gain and thermal noise density are the same in every UMTS system.

The link budget gives a cell range and cell coverage area can be calculated from this range.

An example of uplink budget calculation is presented in **table 2.1**.

The value of total available path loss gives the maximum path loss between the mobile and base station antennas. Log-normal fading margin and indoor/in-vehicle loss are needed to guarantee indoor coverage also in presence of shadowing. Shadowing is caused by buildings, hills, etc. and is modeled as log-normal fading.

The cell range R is calculated from link budget calculations for a certain propagation model, for example, the Okumura-Hata model.

| UMTS UL Link Budget Example | |
|---|---|
| **TX** | |
| Mobile maximum power = 0.125 w (dBm) | 21 |
| Body loss- antenna gain (dB) | 2 |
| EIRP (dBm) | **19** |
| **RX** | |
| BTS noise density (dBm/Hz)= Thermal noise density + BTS noise figure | -168 |
| RX noise power (dBm)= 168+10*log(3840000) | -102,2 |
| Interference margin (dB) | 3 |
| RX Interference power (dBm)= 10*log(10^((-102,2+3)/10)-10^(-102,2/10)) | -102,2 |
| Noise & Interference (dBm)= 10*log(10^((-102,2)/10)+10^(-102,2/10)) | -99,2 |
| Process gain (dB), 144k voice= 10*log(3840/144) | 14,3 |
| Required $Eb/N_0$ for speech (dB) | 5 |
| Antenna gain (dBi) | 19 |
| Cable and connector losses (dB) | 2 |
| Fast fading margin (dB)= slow moving mobile | 4 |
| RX sensitivity (dBm) | **-121,4** |
| Total available path loss (dB) | 140,4 |
| **Dimensioning** | |
| Log normal fading margin (dB) | 7 |
| Indoor/in-vehicle loss (dB) | 0 |
| Soft handover gain (dB) | 3 |
| Cell edge target propagation loss (dB) | 136,4 |
| Okumura-Hata cell range (Km) L=137,4+35,2*log(R) | 0,94 |
| Site hexagon coverage area ($Km^2$) | 2,3 |
| Coverage overlap for handovers (%) | 20 |
| Required suburban coverage area ($Km^2$) | 200 |
| Required suburban coverage sites | 105 |

**Table 2.1** Link budget calculation example

Another step in the radio link budget calculations is estimate the amount of supported traffic per base station site, what is known as load factor.

Uplink load factor can be calculated from the **Equation (2.1)**:

$$\eta ul = (1+i)\cdot\sum_{j=1}^{N} Lj = (1+i)\sum_{j=1}^{N}\frac{1}{1+\frac{W}{(Eb/No)j\cdot Rj\cdot vj}} \qquad \textbf{(2.1)}$$

where:

- $i$ is the ratio of other cell to own cell interference
- $N$ is the number of users per cell
- $Lj$ is the load factor for one connection.
- $W$ is the W-CDMA chip rate (3,84Mcps)
- $Rj$ is the bit rate of the user j. it depends on the service.
- $Vj$ is the activity factor of the user j at the physical layer.
- $Eb/N_0$ is the signal energy per bit divided by the spectrum noise energy that is required to meet a predefined QoS.

The required $Eb/N_0$ can be derived from link level simulations, measurements and 3GPP performance requirements. This includes the effect of the closed-loop power control and soft handover.

The downlink load factor is calculated by using the **Equation (2.2)**:

$$\overline{\eta dl} = \sum_{j=1}^{N} vj \cdot \frac{(Eb/No)j}{W/Rj} \cdot \left[\left(1-\bar{\alpha}\right)+\bar{i}\right] \quad \textbf{(2.2)}$$

where:

- $\bar{i}$ is the average ratio of other cell to own cell base station received power by user.
- $\bar{\alpha}$ is the average orthogonality factor in the cell.

The orthogonality factor is the most important new downlink parameter. Orthogonal codes are used to separate users and without multipath propagation, orthogonality remains when the signal from the base station is received for the mobile. However, if there is enough delay spread in the radio channel, the mobile can see part of this signal from the base station as multiple access interference.

## 2.1.2 CAPACITY UPGRADE PATHS

When the amount of traffic increases, downlink capacity can be upgraded in several ways, such as placing more power amplifiers if the power amplifier is initially split between sectors, using two or more carriers if operator frequency allocation permits, or by means of transmit diversity using a second power amplifier per sector.

## 2.1.3 SOFT CAPACITY

The maximum traffic density that can be supported with a given blocking probability can be calculated in Erlangs basing on the number of channels per cell, as can be seen in the **equation (2.3)**.

$$Traffic\_density[Erlang] = \frac{Call\_arrival\_rate[calls/s]}{Call\_departure\_rate[calls/s]} \quad \textbf{(2.3)}$$

Soft capacity can be explained like this: the lower interference among neighbor cells, the more available channels in the middle of the cell. With few channels per cell, the average load must be quite low in order to guarantee low blocking probability. If the average load is low, there is an extra available capacity in the neighbor channels. These neighbor channels can borrow the extra capacity giving soft capacity because of interference sharing.

W-CDMA soft capacity is defined as the increase of Erlang capacity with soft blocking compares with the increase with hard blocking, considering the same average maximum number of channels per cell for both blockings

$$Soft\_capacity = \frac{Erlang\_capacity\_with\_soft\_blocking}{Erlang\_capacity\_with\_hard\_blocking} - 1 \quad \textbf{(2.4)}$$

## 2.2 CAPACITY AND COVERAGE PLANNING

In this planning process the first step to follow is an iterative prediction of coverage and capacity. An iterative process is needed because all users are sharing the same resources in the air interface and each one is influenced for the others, changing their transmission powers, which affects to more parameters at the same time.

The planning tool for a third generation system must have coverage optimization, interference planning and capacity analysis. Base station configurations optimization and antenna selections, directions and sites optimization are needed in order to get the best quality of service and capacity at the minimum cost. Another needed quality for this tool is the knowledge of radio resource algorithms.

The inputs for this process are real time propagation data for the planned area, estimated user traffic and density and information of existing base station sites. The obtained outputs are the base station locations, their configurations and parameters.

### 2.2.1 UPLINK AND DOWNLINK ITERATION

The uplink iteration aim is to allocate the simulated mobile station transmission powers in such a way that interference levels and base station sensitivity values converge. The downlink load impact in the sensitivity is taken in

account in the term $-10\log(1-\eta_{UL})$. Base station transmission powers are estimated with the sensitivity levels of the best server, the service, the speed and the link losses. These powers are compared with the maximum allowed transmission powers for the mobile stations. The mobile stations that exceed this limit are outage. Interferences are then re-estimated as well as load and sensitivity values for the assigned base stations. If the uplink load factor is higher than the established limit, the mobile stations are randomly moved from the most loaded cell to another carrier or are outage.

The downlink iteration aim is to allocate correctly the base station transmission powers for each mobile station until the received signal from the mobile stations arises the required $Eb/N_0$ target.

## 2.2.2 NETWORK OPTIMIZATION

Network optimization is a process to improve the network global quality and to ensure that the resources are used efficiently.

The process consists of performance measurements, measurement results analysis and updates in network configurations and parameters. Typical network performance measurements are shown in **figure 2.1**. The measurements can be obtained from the test mobile and from the radio network elements.

- Obtained measurements from the test mobile:
  - Uplink transmit power
  - Soft handover rates and probabilities
  - CPICH $Eb/N_0$ and downlink B.L.E.R.
- Obtained measurements from the radio network elements:
  - Connection level measurements: uplink B.L.E.R. and downlink transmit power

- Cell level measurements

It is important to accelerate the measurements analysis. Therefore, the most important results are defined. They are called Key Performance Indicators (KPIs) and can be, for example, base station transmit power, soft handover overhead, drop call rate and packet data delay.

The network tuning can include updates of Radio Resource Management (RRM) parameters: handover parameters, common channel powers, packet data parameters and antenna direction changes.

With the advanced Operations Support System (OSS), network performance monitoring and optimization can be automated. OSS can point out the performance problems, to propose correction actions and also to make some tuning actions automatically.

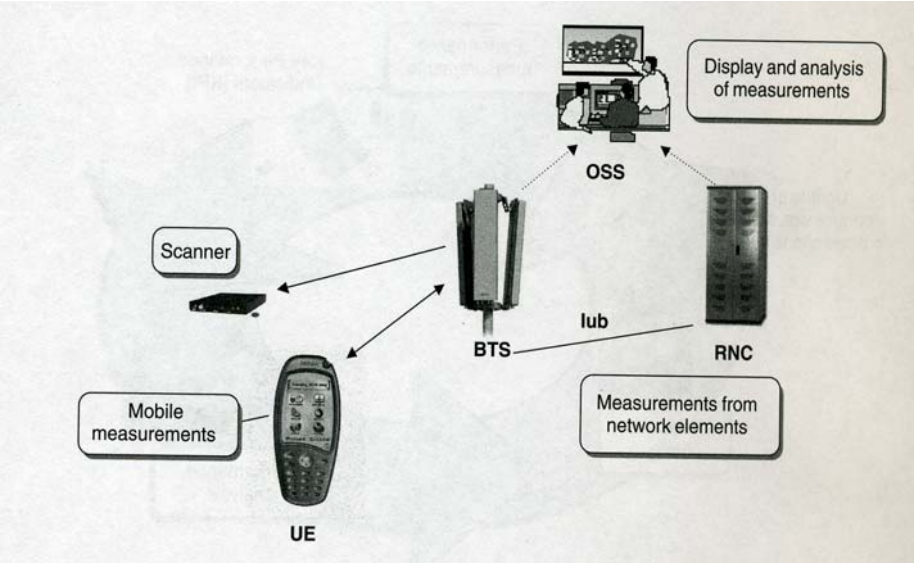


**Figure 2.1** Network performance measurements

## 2.3 GSM CO-PLANNING

In order to accelerate the W-CDMA deployment and to share transmission costs with the existing second generation system, it is necessary to use the existing base station sites.

The feasibility to share sites depends on the existing network relative coverage compared with W-CDMA.

**Table 2.2** shows a comparison of the uplink relative coverage between the existing GSM900 and GSM1800 full-rate voice services and the W-CDMA 64k and 144k data services.

The following conclusions are obtained from this table:

- A W-CDMA 144k data service can be providing by using GSM1800 sites with the same coverage probability than GSM1800 voice service because the maximum path loss is the same.
- If GSM900 sites are used for W-CDMA and full coverage for 64k service is required, a 3 dB coverage improvement is needed in W-CDMA.
- Co-sited W-CDMA and GSM systems can share the antenna when a dual band or a wideband antenna is used. This idea is attractive under the point of view of site solution but it limits the flexibility in the antenna directions optimization for GSM and W-CDMA independently.
- Another co-siting solution is to use separate antennas for the two networks. This solution gives total flexibility to optimize the two networks independently. **Figure 2.2** shows the different co-sitting solutions for GSM and W-CDMA.

| | GSM900/ speech | GSM1800/ speech | W-CDMA/ speech | W-CDMA/ 64 Kbps | W-CDMA/ 144 Kbps |
|---|---|---|---|---|---|
| Mobile transmission power | 33 dBm | 30 dBm | 21 dBm | 21 dBm | 21 dBm |
| Receiver sensitivity | -110 dBm | -110 dBm | -125 dBm | -120 dBm | -117 dBm |
| Interference margin | 1 dB | 0 dB | 2 dB | 2 dB | 2 dB |
| Fast fading margin | 2 dB | 2 dB | 2 dB | 2 dB | 2 dB |
| Base station antenna gain | 16 dBi | 18 dBi | 18 dBi | 18 dBi | 18 dBi |
| Mobile antenna gain | 0 dBi | 0 dBi | 0 dBi | 2 dBi | 2 dBi |
| Body loss | 3 dB | 3 dB | 3 dB | - | - |
| Relative gain from lower frequency compared to UMTS frequency | 7 dB | 1 dB | - | - | - |
| **Maximum path loss** | **160 dB** | **154 dB** | **157 dB** | **157 dB** | **154 dB** |

**Table 2.2** Typical maximum path losses with existing GSM and with W-CDMA

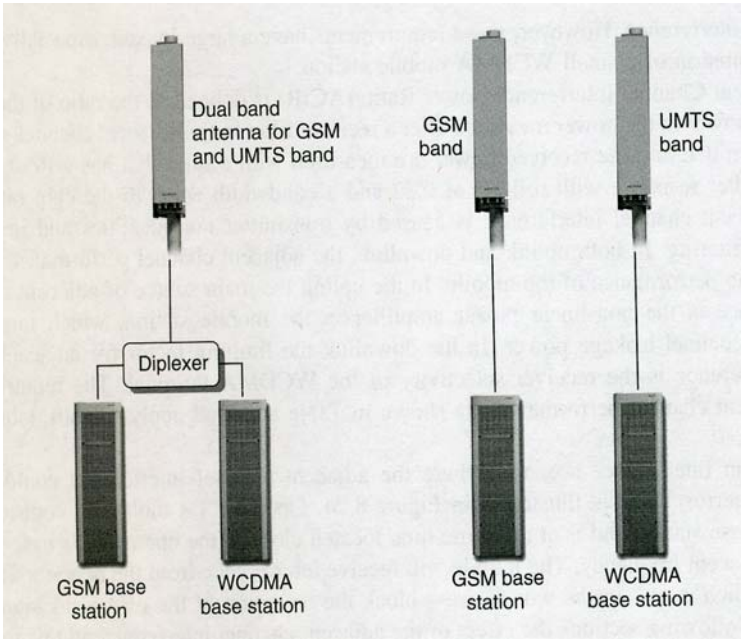


**Figure 2.2** Co-siting of GSM and W-CDMA

# CHAPTER III

# PHYSICAL LAYER PERFORMANCE

In this chapter, the effect of propagation environment, base station solutions and W-CDMA physical layer parameters in coverage and capacity will be studied.

## 3.1 COVERAGE

The effect in the coverage is important during the initial network deployment, as in this moment, the base station site can not collect enough traffic to use the available operator's spectrum completely.

The following equation is used in order to calculate the link budget improvements effect in the maximum cell coverage area:

$$\Delta L\_[dB] = 35.2 \cdot \log\left(1 + \frac{\Delta R}{R}\right) \qquad \textbf{(3.1)}$$

where:

- $\Delta L\ [dB]$ is the effect of the link budget improvements
- $\Delta R/R$ is the relative cell radius. $R$ is the initial cell range and $\Delta R$ is the cell range increase.
- The path loss exponent is 35.2 (a propagation model as the Okumura-Hata model is assumed).

The relative cell area is calculated as:

$$\frac{\Delta A}{A} = \left(1 + \frac{\Delta R}{R}\right)^2 = (10^{\Delta L/35.2})^2 \qquad \textbf{(3.2)}$$

**Table 3.1** shows the relative number of needed base station sites for every link budget improvement. It can be seen that the needed base station density is inversely proportional to the cell area.

| Link Budget Improvement | Relative sites number |
|---|---|
| **0 dB (reference case)** | 100% |
| **1 dB** | 88% |
| **2 dB** | 77% |
| **3 dB** | 68% |
| **4 dB** | 59% |
| **5 dB** | 52% |
| **6 dB** | 46% |
| **10 dB** | 27% |

**Table 3.1** Required relative base station site density reduction with an improved link budget

## 3.1.1 UPLINK COVERAGE

The factors affecting to uplink coverage are:

**1) Bit rate**

The higher bit rates, the lower is the processing gain and the smaller is the coverage.

The processing gain is calculated as:

$$k = 10 \cdot \log\left(\frac{3.84 Mcps}{Tasa\_de\_bit}\right) \qquad \textbf{(3.3)}$$

**Figure 3.1** shows the typical relative coverage for different bit rates. The same maximum mobile station power and sub-urban propagation model are assumed for all bit rates.

Conclusion: wide area uplink coverage will be complicated in UMTS and to provide full uplink coverage at 2 Mbps requires a high base station sites density.

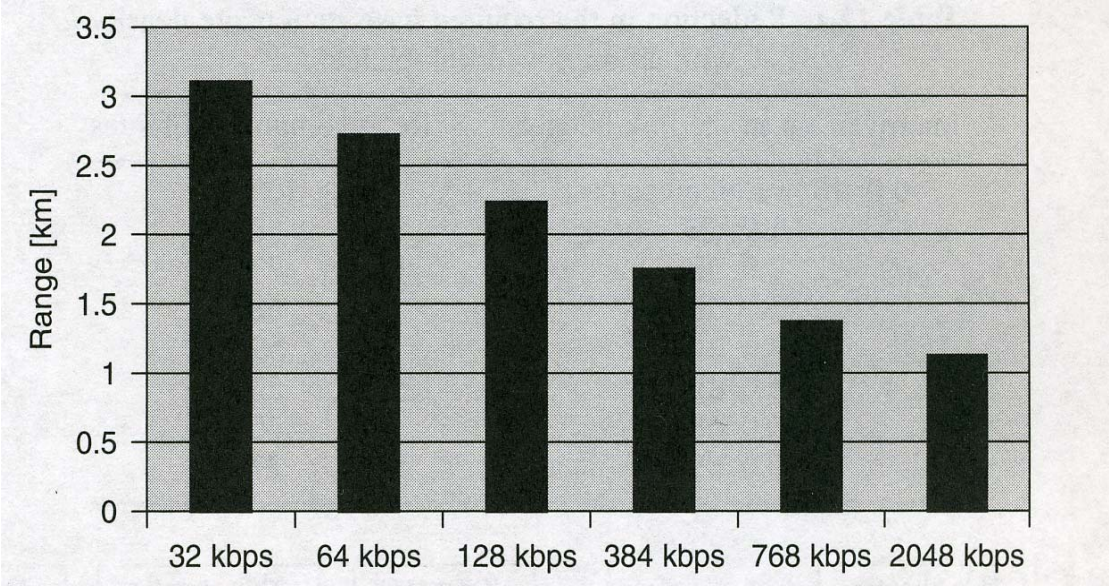


**Figure 3.1** Uplink range of different data rates in suburban area

**2) Adaptative Multirate Speech Codec**

With an Adaptative Multirate (AMR) speech codec is possible to switch to a lower bit rate if the mobile is moving out to the cell coverage area.
The link budget gain reducing the AMR bit rate can be calculated as:

$$Coverage\_gain = 10 \cdot \log\left(\frac{DPDCH(12.2Kbps) + DPCCH}{DPDCH(AMR\_bit\_rate[Kbps] + DPCCH}\right) \quad \textbf{(3.4)}$$

where the power difference between DPCCH and DPDCH is assumed as –3 dB for 12.2 Kbps AMR speech.

For different AMR bit rates, the DPCCH power is kept constant whereas the DPDCH power is changed according to the bit rate. The total transmit power reduction is calculated with the equation 3.4 and can be used to provide a wide uplink cell range.

**Figure 3.2** shows relative cell ranges for different AMR bit rates.

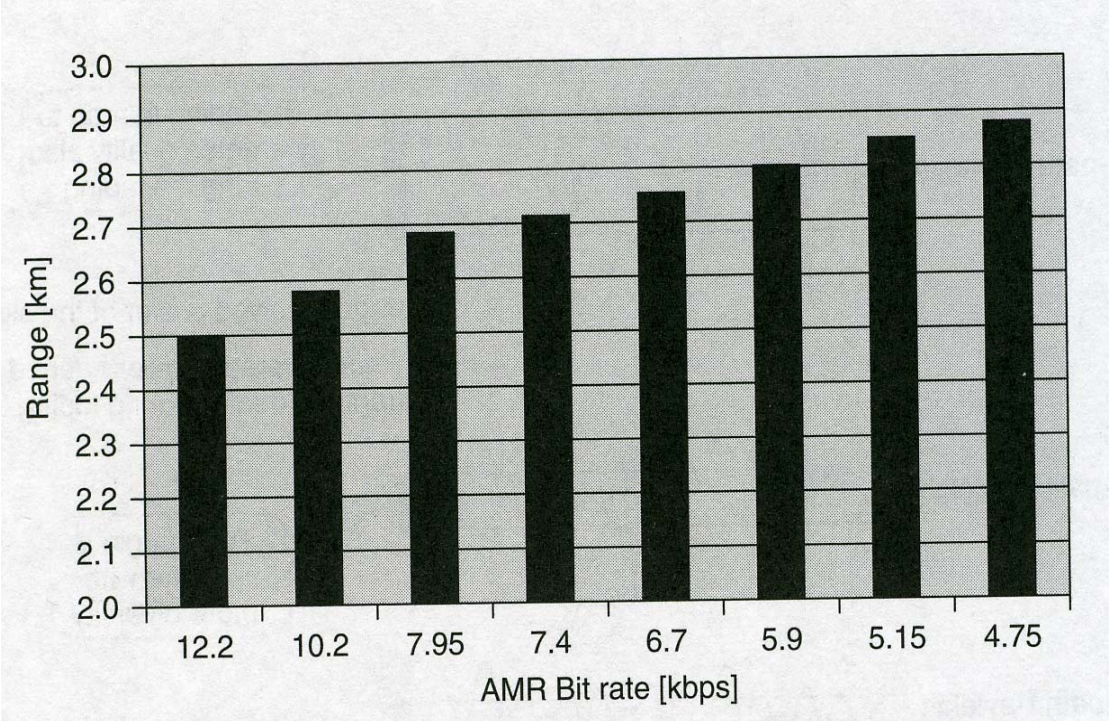


**Figure 3.2** Relative uplink range of different AMR speech codec bit rates

**3) Multipath diversity**

Diversity reduces the signal fading and the required fading margin. The smaller is the required fading margin, better is the coverage.

**4) Soft handover**

During soft handover, the uplink transmission from the mobile is received for two or more base stations. Since there are at least two base stations trying to detect the transmission from the mobile, the probability to detect the signal properly increases.

**5) Receive antenna diversity**

A 3 dB coverage gain can be obtained with receive antenna diversity even if the antenna diversity branches have completely correlated fading. This is because the signals from the two antennas can be combined coherently whereas the receptor thermal noise is combined incoherently.

The 3 dB gain assumes ideal channel estimation in the coherent combination. This gain is achieved because there is more than one receptor branch collecting energy.

Antenna diversity provides also gain against fast fading, as fast fading is typically uncorrelated between the diversity antennas.

There are two ways to obtain receive antenna diversity: space diversity and polarization diversity. They are shown in **figure 3.3**.

**6) Baseband base station algorithms**

Channel estimation accuracy and S.I.R. are important for the receptor $Eb/N_0$. The channel estimation can be improved averaging the estimation over several groups of pilot symbols in the DPCCH and using modulated symbols in DPCCH and DPDCH with decision feedback as additional pilot.

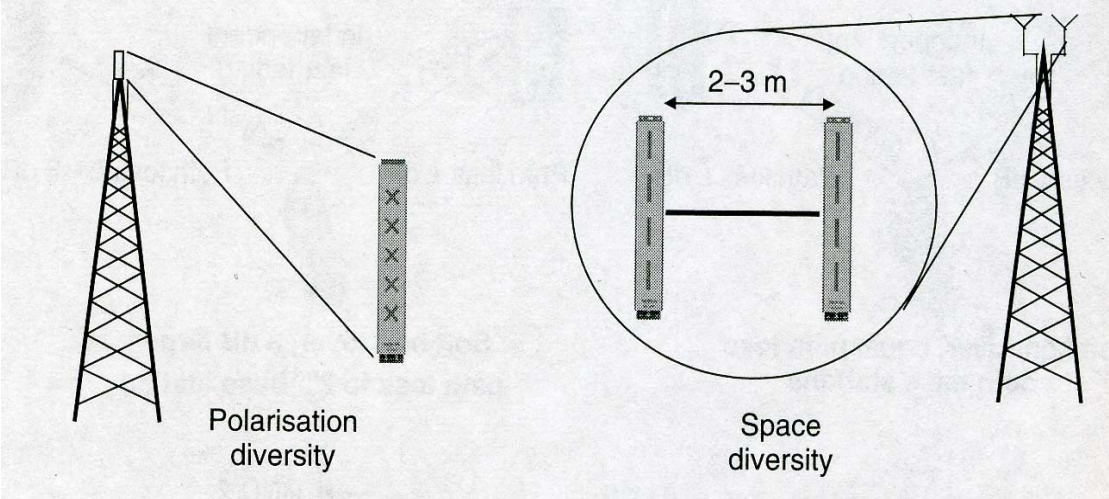


**Figure 3.3** Polarization and space diversity antennas

## 3.1.2 RANDOM ACCESS CHANNEL COVERAGE

The coverage performance for dedicated channels and RACH is different for several reasons. These reasons are shown in **table 3.2**.

Dedicated channels with high bit rate have clearly smaller coverage than RACH. Therefore, RACH coverage needs to be proved against dedicated channels with low bit rate.

| | DCH | RACH |
|---|---|---|
| **Bit rate** | Minimum AMR bit rate: 4.75 Kbps<br><br>Minimum data packet: 2 Mbps | Initial RACH message 2 octets which corresponds to 16 Kbps (10 ms interleaving)<br>8 Kbps (20 ms interleaving) |
| **Soft handover (macro diversity gain)** | 0.8-4 dB | Soft handover not possible |
| **$Eb/N_0$ performance** | - Continuous transmission makes optimized reception easier than with RACH<br>- Coding rate 1/3 | - Short 10 ms or 2 ms burst makes optimized reception difficult<br>- Coding rate ½ |
| **F.E.R. requirements** | Speech 1% | Preferably 10% or below. |

**Table 3.2** Reasons for different coverage of DCH and RACH

The RACH options to match with the coverage of dedicated channels are 20 ms interleaving for DCH bit rate lower than 12.2 Kbps and 10 ms interleaving for DCH bit rate higher then 12.2 Kbps. The 20 ms RACH option should be used only in big cells to improve the RACH coverage. The $Eb/N_0$ is worse for 20 ms RACH than for 10 ms RACH. Therefore, 10 ms option is better for uplink coverage.

## 3.1.3 DOWNLINK COVERAGE

Typical base station power is established at 20 W and mobile station power at 125 mW. With high bit rates, the number of simultaneous connections is low and it is possible to allocate a high power per connection in downlink. Therefore, better coverage for high speed services can be offer in downlink than in uplink.

Assumptions in downlink coverage calculations:

- It is assumed that the total base station power, excluding the common channels, can be allocated for a single user.
- Assumptions in **table 3.3**.

| | |
|---|---|
| *$I_{or}/I_{oc}$ at the cell edge in macro cells* | *-2.5 when other cells high loaded*<br>*3 dB when other cells low loaded* |
| *$I_{or}/I_{oc}$ at the cell edge in micro cells* | *0 dB* |
| *Channel type* | *DCH with soft handover* |
| *$Eb/N_0$* | *5 dB* |
| *B.L.E.R.* | *10%* |
| *Common channels* | *15% of max base station power*<br>*20-25% for 5-10 W base stations in large cells* |
| *Maximum base station power* | *20 W* |
| *Base station cable loss* | *4 dB* |
| *Base station antenna gain* | *18 dBi* |
| *Mobile antenna gain* | *2dBi* |
| *Mobile noise figure* | *7 dB* |
| *Orthogonality* | *Macro cells 0.5*<br>*Micro cells 0.9* |
| *Maximum path loss* | *Macro cell 156 dB*<br>*Micro cell 146 dB* |
| *Path loss exponent* | *3.5* |

**Table 3.3** Assumptions in downlink coverage calculations

The results are shown in **table 3.4**. The macro cell calculations assume 20 W base station power and big cell size.

| | Maximum bit rate at the cell edge | Median bit rate | Area coverage of 384 Kbps |
|---|---|---|---|
| Micro cells | 820 Kbps | 2 Mbps | 100% |
| Macro cells | 350-660 Kbps | 0.8-1.2 Mbps | 92-100% |

**Table 3.4** Downlink coverage results

The effect of the base station output power between 5 and 40 W and the effect of the cell size between 140 and 156 dB can be seen in **figure 3.4**

- 156 dB corresponds to maximum uplink path losses for 64 Kbps with mast head amplifier and 3 dB interference margin.
- 150 dB corresponds to maximum path losses for 128 Kbps with 3 dB cable losses and 3 dB interference margin.
- 140 dB refers a small urban macro cell where 384 Kbps can be offered also in uplink.

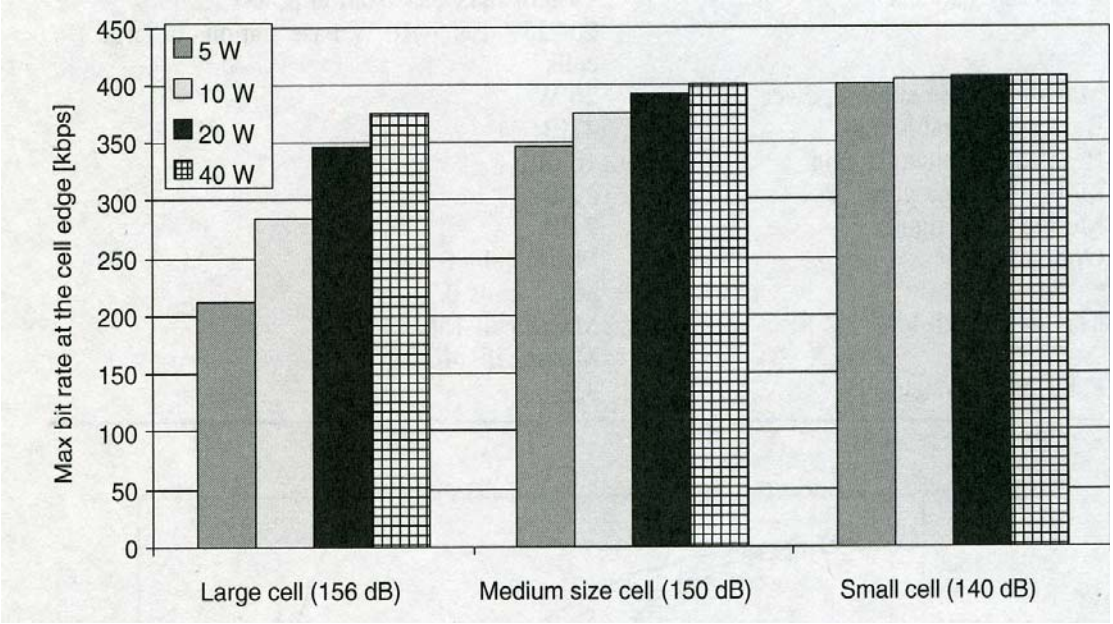


**Figure 3.4** Downlink bit rate at the cell edge with different cell sizes and base station powers

Result conclusions:

- Base station at 5 W provides the same coverage in downlink than at 40 W in small cells.

- With 150 dB, 40 W provides bit rates 15% higher than 5 W and 77% higher in big cells.

### 3.1.4 COVERAGE IMPROVEMENTS

An uplink coverage improvement of W-CDMA base station sites can be reached following these approaches:

- To reduce $Eb/N_0$ increasing the number of receive antennas.
- To reduce cable losses between antenna and the base station low noise amplifier or to add a mast head amplifier.
- To reduce the interference margin.
- To increase the antenna gain with sectorization.

## 3.2 CAPACITY

The air interface capacity in downlink is less than in uplink because better receiver techniques can be use in the base station than in the mobile station. Besides, downlink capacity is more important than uplink capacity because of the asymmetric traffic. These receiver techniques include receiver antenna diversity and multi-user detection.

### 3.2.1 DOWNLINK ORTHOGONAL CODES

**1) Downlink multipath diversity gain**

In a multipath channel, orthogonality is partly lost and intra-cell users interfere to each other.

Let see an example about the downlink performance for the following multipath profiles: ITU Vehicular A, which does no give quite multipath diversity

and ITU Pedestrian A, which gives a significant multipath diversity degree. Both are studied for 8 Kbps with 10 ms interleaving and 1% B.L.E.R.

The simulation scenario and the multipath propagation effect are shown in **figure 3.5** and **figure 3.6** respectively.

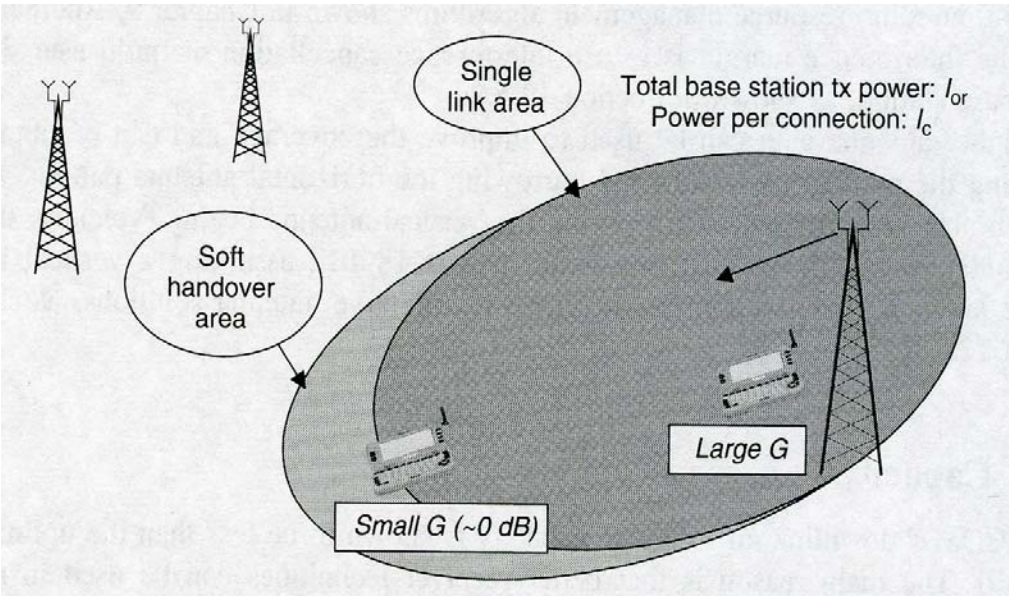


**Figure 3.5** Simulation scenario for downlink performance evaluation

The vertical axis in figure 3.7 shows the required transmission power for speech connection ($I_c$) compares with the total base station power ($I_{or}$) and the horizontal axis shows the total base station power ($I_{or}$) compared with the received interference from the other cells, including the thermal noise ($I_{oc}$). This ratio is called geometric factor G. High G value means that the mobile is closed to the base station and low G value means that the mobile is at the cell edge.

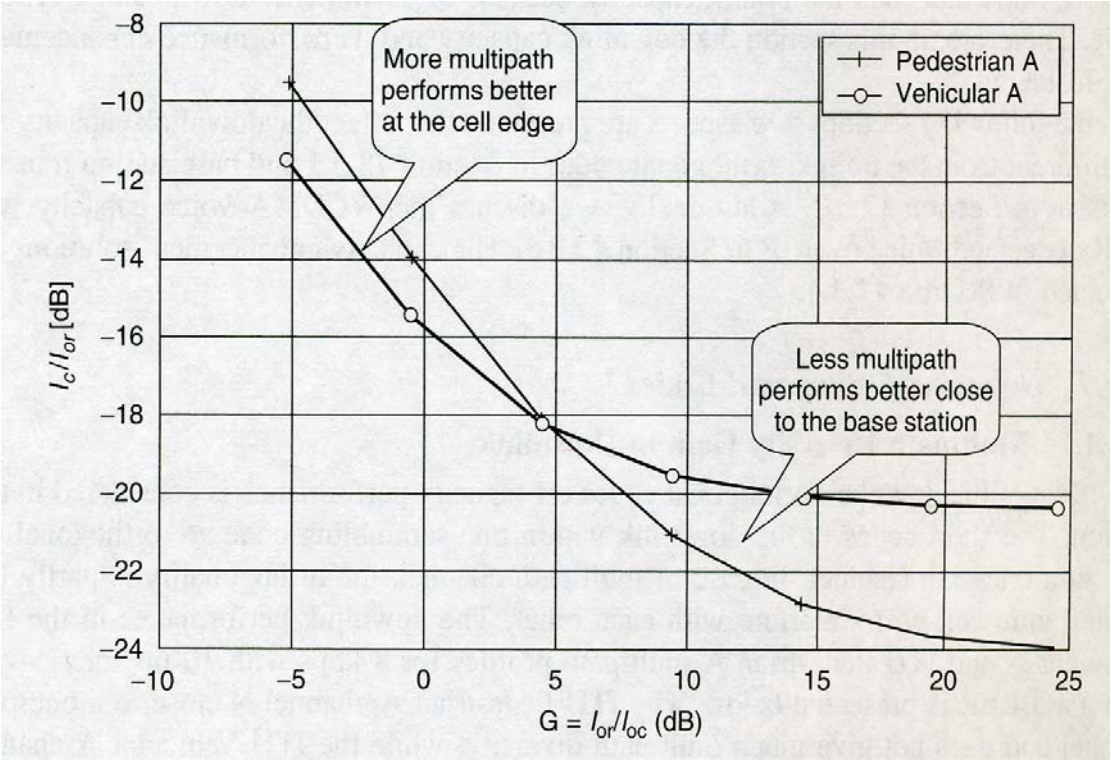


**Figure 3.6** Effect of multipath propagation

The results show that for low G values (at the cell edge) the multipath diversity in the Vehicular channel gives better performance than in the Pedestrian channel. On the other hand, for high G values (closed mobile to the base station) the performance is better in the Pedestrian channel.

Downlink multipath propagation is not beneficial because it reduces orthogonality. Orthogonality loss is the limitation in the W-CDMA receiver design and its performance could be improved with interference cancellation receivers or equalizers in the mobile.

**2) Downlink capacity in different environments.**

The effect of inter-cell interference from adjacent base stations is quite important in downlink capacity. The amount of interference from the adjacent cells depends on propagation environment and the network planning.

The throughput calculation assumptions and the results are shown in **table 3.5** and **table 3.6** respectively.

| | Macro cell | Micro cell |
|---|---|---|
| Downlink orthogonality | 0,5 | 0,9 |
| Other-to-own cell interference ratio i | 0,65 | 0,4 |
| Uplink $Eb/N_0$ | 1,5 dB | 1,5 dB |
| Uplink loading | 60% | 60% |
| Downlink $Eb/N_{0,}$ no transmit diversity | 5 dB | 6,5 dB |
| Downlink loading | 80% | 80% |
| Downlink common channels | 15% | 15% |
| B.L.E.R. | 10% | 10% |

**Table 3.5** Assumptions in the throughput calculations

| | Macro cell | Micro cell |
|---|---|---|
| Uplink | 910 Kbps | 1070 Kbps |
| Downlink | 650 Kbps | 1050 Kbps |

**Table 3.6** Data throughput in macro and micro cell environments per sector per carrier

**3) Number of orthogonal codes**

The number of downlink orthogonal codes is limited into a scrambling code. The maximum number of orthogonal codes is the spreading factor SF. This limitation can affect to the downlink capacity if the environment is favorable and the network hardware and planning support such high capacity.

The downlink achievable capacity with a set of orthogonal codes has been calculated. The calculation assumptions can be seen in **table 3.7** and the results in **table 3.8**.

| Common channels | 10 codes with SF=128 |
|---|---|
| Soft handover overhead | 20% |
| SF for half-rate speech | 256 |
| SF for full-rate speech | 128 |
| Chip rate | 3.84 Mcps |
| Modulation | QPSK (2 bits per symbol) |
| Average DPCCH overhead for data | 10% |
| Channel coding rate for data | 1/3 with 30% puncturing |

**Table 3.7** Assumptions in the calculation of maximum downlink capacity

| | | |
|---|---|---|
| Speech, full rate (AMR 12.2 Kbps and 10.2 Kbps) | **128 channels**<br>***(128-10)/128**<br>**/1.2**<br>**=** 98 channels | **Number of codes with spreading factor of 128**<br>**Common channel overhead**<br>**Soft handover overhead** |
| **Speech, half rate (AMR≤7.95 Kbps)** | 2*98 channels<br>**= 196 channels** | Spreading factor of 256 |
| **Packet data** | 3.84e6<br>*(128-10)/128<br>/1.2<br>*2<br>*0.9<br>/3<br>/(1-0,3)<br>**= 2.5 Mbps** | Chip rate<br>Common channel overhead<br>Soft handover overhead<br>QPSK modulation<br>DPCCH overhead<br>1/3 rate channel coding<br>30% puncturing |

**Table 3.8** Maximum downlink capacity with one scrambling code per sector

## 3.2.2 DOWNLINK TRANSMIT DIVERSITY

The W-CDMA standard supports the use of base station transmit diversity. The transmit diversity aim is to move the antenna diversity complexity from the mobile reception to the base station transmission.

With transmit diversity, the downlink signal is transmitted via two base station antenna branches. The downlink transmit diversity can use space diversity or polarization diversity antennas.

The performance gain from the transmit diversity can be divided in two parts:

1) Coherent combination gain: It can be obtained because the signal is combined coherently whereas the interference is combined incoherently. The ideal coherent combination gain is 3 dB with both antennas. With downlink transmit diversity it is possible to obtain coherent combination in the mobile reception if the phases of the two antennas are adjusted according to the mobile feedback commands in the closed-loop transmit diversity.
2) Diversity gain against fast fading: open-loop and closed-loop transmit diversity give gain against fading because fast fading is uncorrelated from the two transmit antennas.

In order to maximize the limited capacity due to the downlink interference, it would be beneficial to avoid the multipath propagation in order to maintain the code orthogonality and to provide diversity with the transmit antenna diversity.

### 3.2.3 CAPACITY IMPROVEMENTS

The W-CDMA base station site capacity can be improved with the following approaches:

1) More carriers: If the operator's frequency allocation permits, the operator could take another carrier in use. W-CDMA supports efficient inter-frequency handovers. Therefore, several carriers can be used in order to balance the load and to increase the capacity per site.

2) Transmit diversity: it improves the downlink capacity depending on the environment multipath diversity degree. The less is the available multipath diversity, the higher is the downlink capacity gain using transmit diversity.
3) Sectorization: it is used to increase the capacity per site. In an ideal case, N sectors give N times more capacity. Sectorization has the drawback that antennas must be replaced and the radio network planning and optimization has to be redone.
4) Lower bit rate codec, for example, AMR speech codec: it improves the speech capacity using a lower bit rate AMR mode. The number of total transmitted user bits does not increase using lower AMR bit rates. Therefore, the number of connections increases whereas the bit rate per user decreases.

# *PART II*

# *RF RECEIVER SYSTEMS*

# *FOR W-CDMA*

# CHAPTER IV

# RF RECEIVER ARCHITECTURES

Complexity, cost, power dissipation and the number of external components have been the primary criteria in selecting receiver architectures. As IC technologies evolve, however, the relative importance of each of these criteria changes, allowing approaches that once seemed impractical to return as plausible solutions.

## 4.1 HETERODYNE RECEIVER

**Figure 4.1** shows the heterodyne receiver structure. This architecture first translate the signal band down to some intermediate frequency (IF), which is usually much lower than the initially received frequency band. Channel selecting filtering is usually done at this IF, which relaxes the requirements o the channel select filter. The choice of the IF is a principal consideration in heterodyne receiver design.

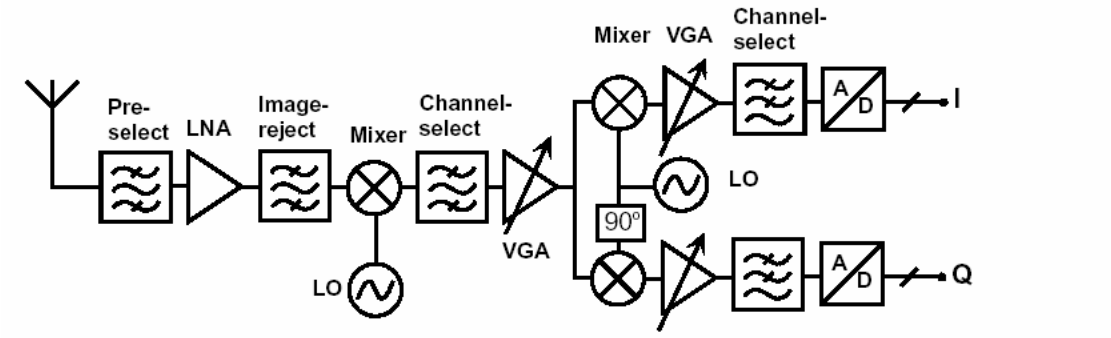


**Figure 4.1** Heterodyne receiver structure

As the first mixer downconverts frequency bands symmetrically located above and below the local oscillator (LO) to the same center frequency, an image-reject filter in front of the mixer is needed. The filter is designed to have a relatively small loss in the desired band and a large attenuation in the image band, two requirements that can be simultaneously meet if $2\omega_{IF}$ is sufficiently large. Thus, a large IF relaxes the requirements for the image-reject filter, which is placed in front of the mixer. On the other hand it complicates the design of the channel-select filter because of the higher IF. In today's cellular systems the channel-select filtering is normally done with surface acoustic wave (SAW) filters.

Another interesting situation arises with an interferer at $(\omega_{wanted} + \omega_{LO})$ /2. If this interferer experiences second-order distortion and the LO contains a significant second harmonic, then a component at $| (\omega_{wanted} + \omega_{LO}) - 2\ \omega_{LO} | = \omega_{IF}$ arises. This phenomenon is called half-IF problem.

A major advantage of the heterodyne receiver structure is its adaptability to many different receiver requirements. That is why it has been the dominant choice in RF systems for many decades. However, the complexity of the structure and the need of a large number of external components (e.g., the IF filter) make problems if a high level of integration is necessary. This is also the major drawback if costs are concerned. Furthermore, amplification at some high IF can cause high power consumption.

# 4.2 HOMODYNE RECEIVER

The homodyne receiver structure (also called zero-IF or direct-conversion architecture) entails vastly different issues from the heterodyne topology. The block diagram is shown in **figure 4.2**. Suppose that the IF in a heterodyne receiver is reduced to zero. The LO will then translate the center of the desired channel to 0 Hz, and the channel translated to the negative frequency half-axis becomes the image to the other half of the same channel translated to the positive frequency half-axis. The downconverted signal must be reconstituted by quadrature downconversion (or some other phasing method), otherwise the negative-frequency half-channel will fold over and superpose on the positive-frequency half-channel.

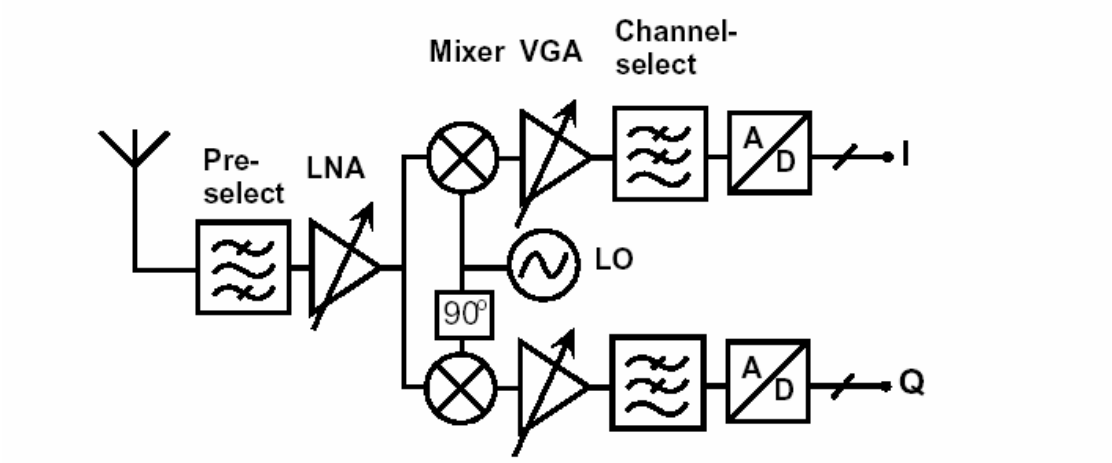


**Figure 4.2** Block diagram of a homodyne receiver

The simplicity of this structure offers two important advantages over a heterodyne counterpart. First the problem of image is circunvented because $\omega_{IF}$ =

0. As a result, no image filter is required. This may also simplify the LNA design, because there is no need for the LNA to drive a 50 Ω load, which is normally necessary when dealing with image-reject filters. Second, the IF SAW filter and subsequent downconversion stages are replaced with low-pass filters and baseband amplifiers that are amenable to monolithic integration. The possibility of changing the bandwidth of the integrated low-pass filters (and thus changing the receiver bandwidth) is a major advantage if multimode and multiband applications are concerned.

On the other hand the zero-IF topology entails a number of issues that do not exist or are not as serious in a heterodyne receiver. Since in a homodyne topology the downconverted band extends to zero frequency, offset voltages can corrupt the signal and, more importantly, saturate the following stages. There are three main possibilities how DC-offsets are generated. First, the isolation between the LO port and the inputs of the mixer and the LNA is not infinite. Therefore, a finite amount of feedthrough exists from the LO port to the mixer or the LNA input. This “LO leakage” arises from capacitive and substrate coupling and, if the LO signal is provided externally, bond wire couplings. This leakage signal is now mixed with the LO signal, thus producing a DC component at the mixer output. This phenomenon is called “self-mixing”. A similar effect occurs if a large interferer leaks from the LNA or mixer input to the LO port and is multiplied by itself. A time varying DC offset is generated if the LO leaks to the antenna and is radiated and subsequently reflected from moving objects back to the receiver.

Large amplitude modulated signals are converted to the baseband section via second order distortion of the IQ-mixers also lead to time varying DC offset. The spectral shape of this signal contains a significant component at DC accounting for approximately 50% of the energy. The rest of the spurious signal

extends to two times of the signal bandwidth before downconverted by the second-order nonlinearity of the mixers. The cause for the large signal content at DC is that every spectral component of the incident interferer is coherently downconverted with itself to DC. In order to prevent this kind of DC offset, a large second-order intercept point (IP2) of the IQ-mixer is necessary.

## 4.3 DIGITAL-IF RECEIVERS

In the heterodyne receiver architecture of figure 4.1 the second downconversion and subsequent filtering can be done digitally. The principal issue in this approach is the performance required from the ADC. To limit the requirement on the ADC, a sufficiently low IF has to be chosen, which make it impossible to employ bandpass filtering to suppress the image frequency. Thus, an image suppression mixer has to be used. The image suppression feasible in today's systems is limited to a range of 30-55 dB. Due to the high demands on the ADC and the image suppression mixer performance this architecture has not been used for terminal applications.

# CHAPTER V

# REQUIREMENTS FOR LOW-NOISE AMPLIFIERS IN WIRELESS COMMUNICATIONS

This chapter treats to point out the challenges in the LNA design for modern telecommunications systems and to justify some of the choices made in circuit design.

# 5.1 DESIGN PARAMETERS FOR LOW-NOISE AMPLIFIERS

This section describes the essential parameters needing in LNA design and explains how these parameters can be calculated from the analog receiver requirements.

## 5.1.1 SENSITIVITY AND NOISE FIGURE

The sensitivity is defined as the minimum signal which has to be detected with a sufficient signal quality determined typically as a bit or frame error rate (B.E.R. / F.E.R.).

$$S_{sensitivity} = -174dBm + 10\log(B) + SNR_{\min} + NF \qquad \textbf{(5.1)}$$

where:

- $-174dBm$ is the available noise power from the source at 290K (k*T).
- $B$ is the channel bandwidth.
- $SNR_{min}$ is the minimum signal-to-noise ratio required to detect the signal with an acceptable B.E.R.
- $NF$ is the noise figure for the receiver.

The required noise figure for W-CDMA can be calculated from the following parameters:

- Total code and spreading gain, $G_{s,c}$ = 25dB.
- Digital baseband implementation margin, $IL_{bb}$ = 2dB.
- Required bit energy to interference power spectral density ratio, $Eb,req/I$ = 5dB.
- Sensitivity level in W-CDMA specification, $S_{sensitivity}$ = -117dBm
- Signal-to-noise ratio before dispreading,

$$SNR = Eb,req/I + IL_{bb} - G_{s,c} = 5dB + 2dB - 25dB = -18dB$$

From equation 5.1, the noise figure can be estimated as:

$$NF = S_{sensitivity} + 174dBm - 10\log(B) - SNR_{\min} \qquad \textbf{(5.2)}$$

Replacing the terms in equation 5.2 by the parameters defined above, the noise figure value for W-CDMA is:

$$NF = -117dBm + 174dBm - 10\log(5*10^6) + 18dB = 9dB$$

The noise figure for the whole receiver describes how much the receiver can deteriorate the signal-to-noise ratio of the received signal.

$$NF = 10\log\left(\frac{\frac{S_{in}}{N_{in}}}{\frac{S_{out}}{N_{out}}}\right) \qquad \textbf{(5.3)}$$

The noise figure for the different blocks can be calculated with the Friis formula:

$$Ftot = F_1 + \frac{F_2 - 1}{G_1} + \frac{F_3 - 1}{G_1 G_2} + \ldots + \frac{F_n - 1}{G_1 G_2 \ldots G_n} \qquad \textbf{(5.4)}$$

$$NFtot = 10\log(Ftot) \qquad \textbf{(5.5)}$$

where:

- $F_n$ and $G_n$ are the noise factor and the available power gain for the nth block.

NF and G are characterized for every block **(figure 5.1)**.

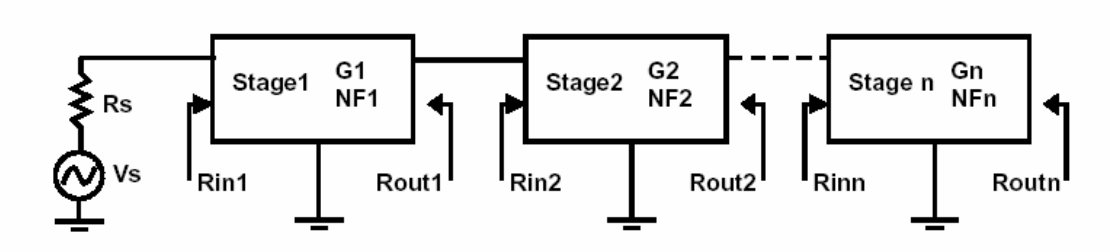


**Figure 5.1** Cascade receiver stages

The available power gain G can be calculated as:

$$G = \frac{v_{outn}{}^2 / 4R_{out}}{v_s{}^2 / 4R_s} \qquad \textbf{(5.6)}$$

where:

- $V_{outn}{}^2/4R_{outn}$ is the power delivered to the conjugated-matched load.
- $V_s{}^2/4R_s$ is the available power from the source delivered to the conjugated-matched circuit.

Friis' formula is useful in the heterodyne receiver due to its off-chip components, which use defined characteristic loads.

In DCRs there is no need to manage off-chip circuits. Thus, it is not necessary to match to certain impedance among different blocks. The signal is transferred typically in voltage mode and in an ideal case the source with zero impedance drives the infinite input impedance of the following block. Therefore, the conversion gains and the noise levels should be defined voltages and impedance levels instead of power.

$$Ftot = F_1 + \frac{F_2 - 1}{A_{0,1}{}^2 A_{v1}{}^2} + \frac{F_3 - 1}{A_{0,1}{}^2 A_{1,2}{}^2 A_{v1}{}^2 A_{v2}{}^2} + \ldots + \frac{F_n}{(A_{0,1}{}^2 \cdot \ldots A_{n-2,n-1}{}^2)(A_{v1}{}^2 \cdot \ldots A_{v2}{}^2)} \quad \textbf{(5.7)}$$

where:

- $A_{vn}$ is the voltage gain of the nth stage at open load.
- $A_{n-2,n-1}$ transforms the impedance among different stages as:

$$A_{n-2,n-1} = \frac{Zin_{,n-1}}{Zin_{,n-1} + Zout_{,n-2}} \quad \textbf{(5.8)}$$

where

- $Z_{in}$ and $Z_{out}$ are the input and the output impedances of the corresponding stages.

In DCRs, the input impedance of the following stage is usually much higher than the output impedance of the precedent stage. Therefore, the term $A_{n-2,n-1}$ can be ignored.

## 5.1.2 LINEARITY

The receiver must be able to detect the desired signal in presence of other interfering signals.

The signal powers at the receiver input can vary between -110dBm and 0dBm. These signals are partly filtered in the pre-select filter but the signals in the reception band pass through the LNA.

The receiver linearity is characterized by means of the gain compression, the third order intercept point (IIP3) and the second order intercept point (IIP2).

#### 5.1.2.1 Gain compression and harmonic distortion

The compression gain determines how large an input signal can be accepted at the receiver input. In RF circuits, the gain compression is defined as "-1-dB compression point", point where the gain decreases 1dB from the gain at small signal levels. In receivers, the compression point is usually referred to the input (ICP).

The harmonic distortion is the magnitude of the ratio between the signal at the nth frequency and the signal at the fundamental frequency. It can be calculated in this way:

- The three first terms for a non-lineal, without memory and time-variant system are:

$$y(t) = \alpha_1 x(t) + \alpha_2 x^2(t) + \alpha_3 x^3(t) \qquad \textbf{(5.9)}$$

- Input signal:

$$x(t) = A\cos(\omega t) \qquad \textbf{(5.10)}$$

- Therefore:

$$y(t) = \frac{\alpha_2 A^2}{2} + \left( \alpha_1 A + \frac{3\alpha_3 A^3}{4} \right) \cos(\omega t) + \frac{\alpha_2 A^2}{2} \cos(2\omega t) + \frac{\alpha_3 A^3}{4} \cos(3\omega t) \quad \textbf{(5.11)}$$

Let notice that the term at the fundamental frequency also depends on the third order term ($\alpha_3$). The output signal is decreased when $\alpha_3$ has opposite sign to $\alpha_1$.

### 5.1.2.2 Third-order intercept point

In this case, two signals with different frequency are using as input to the non-lineal, without memory and time-variant system.

$$x(t) = A\cos(\omega_1 t) + B\cos(\omega_2 t) \quad \textbf{(5.12)}$$

The output is:

$$\begin{aligned} y(t) = {} & \frac{1}{2}\alpha_2 (A^2 + B^2) + \alpha_1 A \cos(\omega_1 t) + \alpha_3 \left( \frac{3}{4} A^3 + \frac{3}{2} AB^2 \right) \cos(\omega_1 t) \\ & + \alpha_1 B \cos(\omega_2 t) + \alpha_3 \left( \frac{3}{4} B^3 + \frac{3}{2} A^2 B \right) \cos(\omega_2 t) + \frac{1}{2}\alpha_2 A^2 \cos(2\omega_1 t) \\ & + \frac{1}{2}\alpha_2 B^2 \cos(2\omega_2 t) + \frac{1}{4}\alpha_3 A^3 \cos(3\omega_1 t) + \frac{1}{4}\alpha_3 B^3 \cos(3\omega_2 t) \\ & + \alpha_2 AB \cos((\omega_1 - \omega_2)t) + \alpha_2 AB \cos((\omega_1 + \omega_2)t) + \frac{3}{4}\alpha_3 A^2 B \cos((2\omega_1 - \omega_2)t) \\ & + \frac{3}{4}\alpha_3 AB^2 \cos((2\omega_2 - \omega_1)t) + \frac{3}{4}\alpha_3 A^2 B \cos((2\omega_1 + \omega_2)t) + \frac{3}{4}\alpha_3 AB^2 \cos((2\omega_2 + \omega_1)t) \end{aligned}$$

**(5.13)**

The most harmful intermodulation products in the LNA design are the frequencies $2f_2 - f_1$ and $2f_1 - f_2$.

The IIP3 requirements for the receiver blocks can be calculated by using the following equation:

$$\frac{1}{iip3_{tot}} = \frac{1}{iip3_1} + \frac{G_1}{iip3_2} + \ldots + \frac{\prod_{i=1}^{n-1} G_i}{iip3_n} \qquad \textbf{(5.14)}$$

where:

- $iip3_n$ is the iip3 magnitude of the nth block.
- $G_n$ is the power gain (magnitude) of the nth block.

This equation assumes that all the spurious signals are at the same phase, giving therefore an assumption of the worst case for the IIP3 result. $G_n$ can be replaced by the square of the voltage gain ($A_v^2$). In addition, in order to get accurate results, the gain should be determined by using suitable source and load impedances. However, the source and the load impedances of the design stage should be lineal in order not to affect to the results. Hence, it would be necessary to model these impedances with lineal components, what it can be difficult in some cases. In DCRs, the channel-select filter is a passive structure and the filtering can lead to a finite IIP3 which should be taken in account in the calculations.

## 5.2 DESIGN OF A SINGLE-SYSTEM LOW-NOISE AMPLIFIER

In this section, the design aims for single-system low-noise amplifiers will be studied, including the design of the input transistor, the load and the biasing. The load for the LNA is implemented on-chip. Hence, matching at the LNA output is no required.

The design methodology has been done in order to achieve a NF as low as possible with an enough bandwidth and linearity for cellular applications. The focus of the section is the single-stage inductively-degenerated common-emitter amplifier. Its configuration is shown in **figure 5.2**.

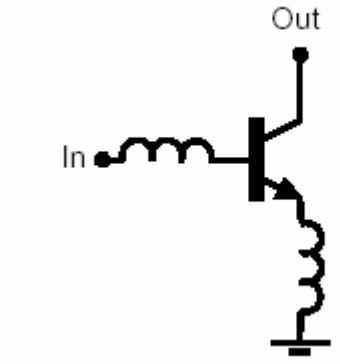


**Figure 5.2** Schematic of an inductively-degenerated LNA

The small-signal model for the bipolar transistor can be seen in **figure 5.3**.

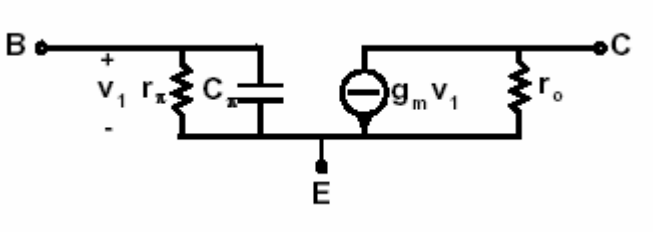


**Figure 5.3** Simplified small-signal model of a bipolar transistor

## 5.2.1 INPUT MATCHING

It is needed because the frequency response of the pre-select filter or balun is valid only for one specific output impedance. Input matching is typically defined by the return losses.

$$S_{11} = 20\log\left(\left|\frac{Z_{IN} - Z_s}{Z_{IN} + Z_s}\right|\right)(dB) \qquad \textbf{(5.15)}$$

where:

- $Z_{IN}$ is the input impedance of the LNA.
- $Z_S$ is the input impedance of the source.

In an inductively-degenerated LNA, the base and emitter inductors are used for matching purposes. The input impedance considering $C_\pi <<< R_\pi$, is:

$$Z_{IN} = \frac{g_{m,T} \cdot L_e}{C_\pi} + j\left(\omega(L_b + L_e) - \frac{1}{\omega C_\pi}\right) \qquad \textbf{(5.16)}$$

This impedance only has real part at the resonance frequency of the series resonator formed by $L_b$, $L_e$ and $C_\pi$.

## 5.2.2 VOLTAGE GAIN

The voltage gain is calculated as:

$$A_v = G_m \cdot \left| Z_L(j\omega) \right| \qquad \textbf{(5.17)}$$

where:

- $Z_L(j\omega)$ is the load impedance of the LNA.
- $G_m$ is the transconductance of the amplifier ( $G_m = \left| I_{out} / v_{in} \right|$ )

The transconductance in an inductively-degenerated LNA is:

$$G_m = \left| \frac{g_m}{\left( \frac{j\omega L_b + j\omega L_e + 1}{j\omega C_\pi} \right) j\omega C_\pi + j\omega L_e g_m} \right| \qquad \textbf{(5.18)}$$

At the resonance frequency, the term between brackets becomes zero and $G_m$ is:

$$G_m = \frac{1}{\omega_r L_e} \qquad \textbf{(5.19)}$$

where:

- $\omega_r$ is the matching angular frequency.

From equation 5.19 it can be noticed that the transconductance can not be adjusted changing the $g_m$ of the transistor without changing the matching.

## 5.2.3 NOISE FIGURE

It determines how the LNA degrades the signal-to-noise ratio. The small-signal model for a bipolar transistor including the most important noise sources is shown in **figure 5.4**.

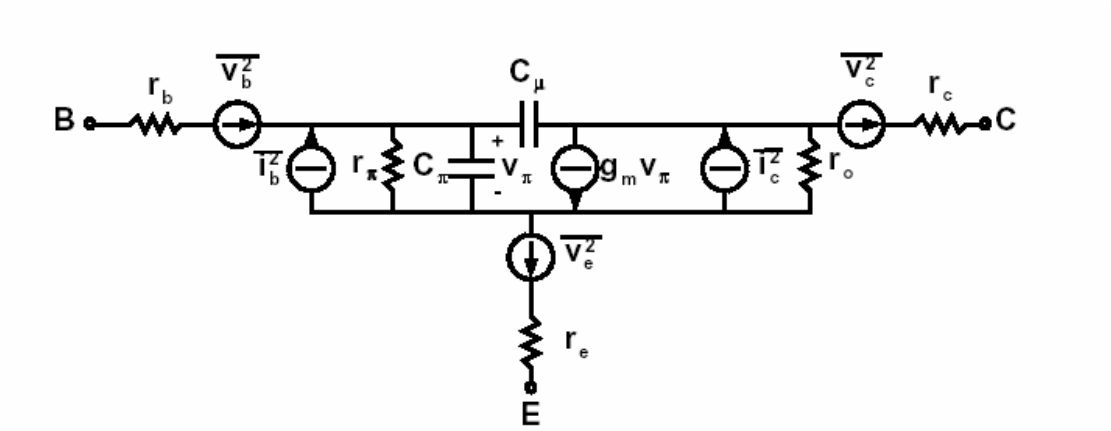


**Figure 5.4** Small-signal model of a bipolar transistor including the noise sources

The minimum achievable NF in a common-emitter when matched to optimum source impedance is:

$$NF_{\min} = 1 + \frac{n}{\beta_{DC}} + \sqrt{\frac{2I_c}{V_T}(r_e + r_b)\left(\frac{f^2}{{f_T}^2} + \frac{1}{\beta_{DC}}\right) + \frac{n^2}{\beta_{DC}}} \qquad \textbf{(5.20)}$$

where:

- $r_e$ and $r_b$ are the emitter and base resistances respectively.
- $I_c$ is the collector current.
- $f_T$ is the unity gain frequency.
- $\beta_{DC}$ is the continuous current gain.

- $n$ is the collector current linearity factor (1-1,2).
- $f$ is the operation frequency.

The value of the optimum source resistor is:

$$R_{s\_opt} = \frac{f_T}{f}\left(\frac{n^2}{2I_c} + (r_e + r_b)\right)\left[\frac{\sqrt{\frac{I_c}{2V_T}(r_e + r_b)\left(1 + \frac{{f_T}^2}{\beta_{DC} \cdot f^2}\right) + \frac{n^2 \cdot {f_T}^2}{4\beta_{DC} \cdot f^2}}}{\frac{I_c}{2V_T}(r_e + r_b)\left(1 + \frac{{f_T}^2}{\beta_{DC} \cdot f^2}\right) + \frac{n^2}{4}\left(1 + \frac{{f_T}^2}{\beta_{DC} \cdot f^2}\right)}\right] \quad \textbf{(5.21)}$$

The optimum NF is achieved by adjusting the collector current of the unit transistor according to equation 5.20. Then, by keeping a constant current through the unit transistor, the number of parallel transistors is increased until the suitable source resistance is achieved.

## 5.2.4 CASCODE TRANSISTOR

The experimental LNAs using in this thesis use cascode transistors between the load and the input transistor **(figure 5.5)**.

This configuration presents several benefits which are especially suitable for DCRs.

- It reduces the Miller effect in the input transistor as the input impedance of the cascode transistor is usually smaller than the load impedance.
- It increases the separation between the LNA input and output terminals compared to a LNA with a single transistor. Hence, the input transistor and the load sizes can be optimized separately when matching.

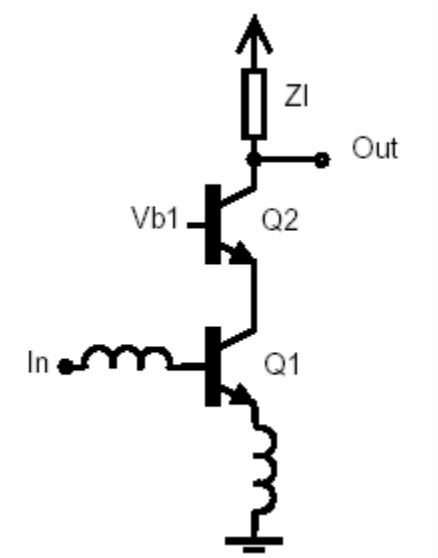


**Figure 5.5** Inductively-degenarated LNA with a cascode transistor

The small signal model of a inductively-degenerated cascode bipolar LNA can be seen in **figure 5.6**.

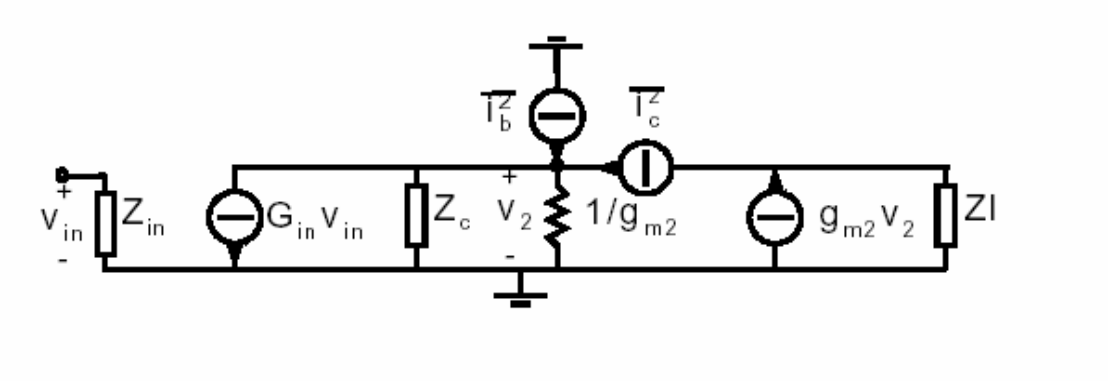


**Figure 5.6** Noise sources of a cascade transistor

where:

- $G_{in}$ is the transconductance of the degenerated input transistor.

- $\overline{i_c^2}$ and $\overline{i_b^2}$ are the collector and base current noise sources of the cascode transistor.
- $Z_c$ is the combination in parallel of all of the impedances in the input transistor collector excluding $1/g_{m2}$.
- $1/g_{m2}$ is the resistor of the cascode transistor.
- $Z_L$ is the load impedance.

Both noise sources are independent so they can be calculated independently. The output noise voltage of the cascode LNA with both noise sources is:

$$\overline{v_{nout}^2} = \left(\frac{1/g_{m2}Z_C}{1+1/g_{m2}Z_c}\right)^2 \overline{i_c^2} \cdot Z_L^2 + \left(\frac{1}{1/g_{m2}Z_C}\right)^2 \overline{i_b^2} Z_L^2 \qquad \textbf{(5.22)}$$

And the voltage gain of the matched cascode LNA is:

$$A_v = G_{in} \frac{1}{1+1/g_{m2}Z_C} Z_L \qquad \textbf{(5.23)}$$

By using equations 5.22 y 5.23, the LNA noise figure is:

$$NF = 10\log\left(F_{in} + \frac{\overline{i_c^2}}{KTBR_s G_{in}^2}\left(1/g_{m2}Z_c\right)^2 + \frac{\overline{i_b^2}}{KTBR_s G_{in}^2}\right) \qquad \textbf{(5.24)}$$

where:

- $F_{in}$ is the noise factor of the input transistor.

The effect of the collector noise in the LNA noise figure depends on the impedance $Z_c$. In order to minimize the noise figure degradation caused by the collector shot noise, $Z_c$ has to be maximized, for example, by using small devices.

The base shot noise has a constant value. This noise can be minimized by selecting the collector current of a unit transistor with the maximum β in order to achieve minimum base current. In addition, the impedance at the collector of the input transistor affects to the LNA voltage gain. The voltage gain can be adjusted by changing the load impedance. However, if the load impedance increases, the load noise increases, as well as the LNA noise figure.

## 5.2.5 LNA LOAD

The possible alternatives for a LNA passive load are studied in this paragraph.

### 5.2.5.1 Resistive load

An ideal resistor has an infinite bandwidth and, compared to loads which use inductors, the resistive load has a small chip area. However, even with an ideal resistor, the LNA output can be assumed as resistive only at low frequencies. At high frequencies, the different capacitors at the LNA output start to limit the usable bandwidth.

In a cascode common-emitter LNA, which drives the quadrature mixers, the output capacitance is the sum of the capacitance at the mixer input, the transistor parasitic capacitance and the parasitic capacitance of the load resistor.

### 5.2.5.2 Resonator load

The basic resonator load consists of a capacitor and an inductor in parallel. With ideal components, it has infinite impedance in an infinitely small bandwidth at the resonance frequency:

$$f_r = \frac{1}{2\pi\sqrt{LC}} \qquad \textbf{(5.25)}$$

Thus, it would be useless in the LNA design.

However, the inductor losses reduce the impedance and increase the resonator bandwidth.

The on-chip inductor differs to the ideal inductor and needs an accurate modeling. The typical model for an on-chip spiral inductor is shown in **figure 5.7**. It has a parasitic capacitance to the ground signal. The serial resistor reduces the inductor losses. Thus, an on-chip inductor forms a resonator with finite impedance.

The simplified model of a cascode LNA using a resonator load is shown is **figure 5.8**.

- The capacitor includes the parasitic capacitance of the inductors, the capacitance of the mixer input, the parasitic capacitance of the cascade transistor and the on-chip capacitance.
- $R_P$ is the parallel on-chip resistor. Its purpose is to adjust the resonator impedance, which is:

$$Z_r(j\omega) = \frac{1}{\frac{1}{R_P} + \frac{R_L}{R_L^2 + \omega^2 L^2} + j\left(\omega C - \frac{\omega L}{R_L^2 + \omega^2 L^2}\right)} \qquad \textbf{(5.26)}$$

- The resonance frequency is:

$$f_r = \frac{1}{\sqrt{LC}}\sqrt{1 - \frac{R_L^2 C}{L}} \qquad \textbf{(5.27)}$$

- And the impedance at the resonance frequency is:

$$Z(f_r) = \frac{1}{\frac{1}{R_P} + \frac{R_L}{R_L^2 + \omega_r^2 L^2}} \qquad \textbf{(5.28)}$$

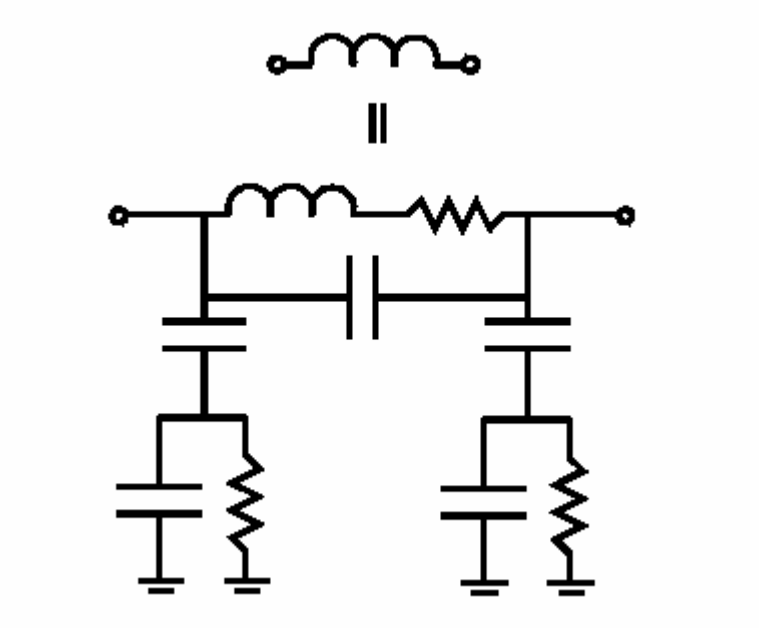

**Figure 5.7** Typical model of a planar inductor

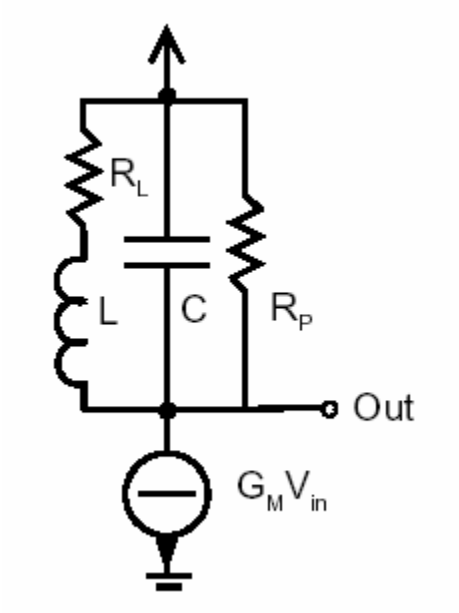


**Figure 5.8** Simplified LNA with a resonator load

Therefore, the resonator impedance can be adjusted with the parallel resistance $R_P$ or with the inductance L. If the value of the inductor is changed, the inductance and the serial resistance also change as well so the capacitance C must be adjusted in order to keep constant the resonance frequency.

The resonator is usually defined by the quality factor, Q, which is defined as the ratio of the stored energy and the dissipated energy per frequency cycle in the system:

$$Q = 2\pi \frac{stored\_energy}{dissipated\_energy\_in\_one\_oscillation\_cycle} \qquad \textbf{(5.29)}$$

It can be also determined by using the -3-dB bandwidth of the resonator:

$$Q = \frac{\omega}{\omega_{-3dB}} \qquad \textbf{(5.30)}$$

$$Q = \frac{R_P(R_L + \omega_r{}^2 L^2)}{(R_L + \omega_r{}^2 L^2 + R_L R_P)\omega_r} \qquad \textbf{(5.31)}$$

If $R_L << \omega_r{}^2 L^2$ then:

$$Q = \frac{R_P \omega_r L}{\omega_r{}^2 L^2 + R_L R_P} \qquad \textbf{(5.32)}$$

When $R_P$ is set to infinity by using equations 5.28 and 5.32, the resonator impedance becomes:

$$Z(f_r) = Q\omega_r L \qquad \textbf{(5.33)}$$

Hence, the maximum gain for the LNA is obtained making the inductance value as maximum as possible. The maximum inductance is rarely used because the resonator capacitor is then formed by the parasitic capacitance at the LNA output and the inductor is operating closed to its self-resonance frequency. Thus, the resonance is sensitive to the process parameters. In addition, large inductance values require more chip area. The DC voltage at the LNA output, when the resonator is being used is, in practice, close to the supply voltage. Therefore, the load does not limit the required supply voltage. In addition, the resonator acts as a low-pass filter. However, the Q value of the resonator must be low enough to cover the whole reception band in all the process. Thus, in practice, the filtering due to the load resonator is only marginal.

## 5.2.6 LNA BIASING

The schematic of the biasing of a inductively-degenerated cascode bipolar LNA can be seen in **figure 5.9**. The current flowing through the LNA is determined by the current mirror formed by the transistors Q1 and Qb1. The impedance Zb1 blocks the leakage of the input signal to the biasing circuit and to the bias voltage Vcas, determines the $V_{CE}$ voltages of the input and cascode transistors.

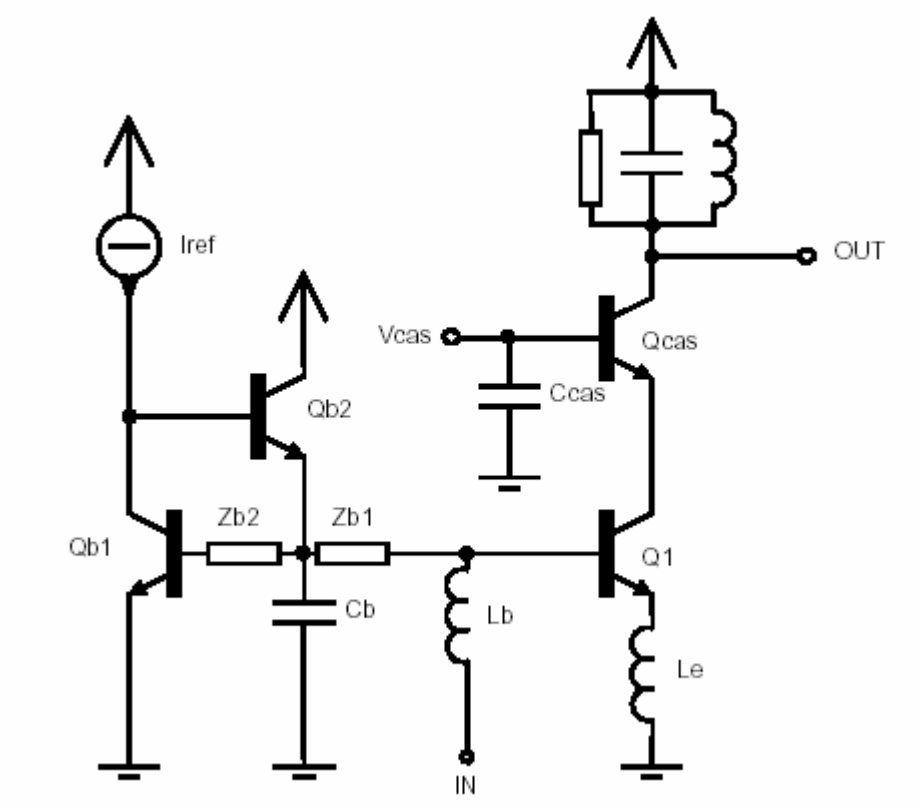


**Figure 5.9** Inductively-degenerated LNA including bias

The solutions for Zb1 y Zb2 in order to get an accurate current mirror are:

- If Zb1 is a resistor, Zb2 has to be also a resistor.

- If Zb1 is an inductor, Zb2 has to be a short circuit as there is no voltage drop in the inductor.

Qb2 increases the accuracy of the current mirror as the required base current for Q1 and Qb1 is not taken from the reference current, Iref. However, it may be necessary to remove Qb2 for lower supply voltages, as the current mirror formed by Q1, Qb1 and Qb2 requires a supply, at least, twice the base-emitter voltage. In addition, if the emitter inductor, Le, is on-chip, the series resistance of the spiral inductor affects to the accuracy of the current mirror.

There are alternative methods for the LNA biasing. For example, the current of Q1 can be fixed by using a current source below Le, connecting a capacitor in parallel to the current source in order to remove the current source noise and to make the node between the current noise and the inductor to the signal ground.

The effect of the different biasing configurations to the LNA performance and the LNA sensitivity to the bias variations with the process parameters must be checked out during the design process.

- An inadequate biasing arrangement can decrease significantly the LNA performance.
- The LNA noise figure increases because the bias noise is not properly filtered out. This can be done by using adequate filtering capacitances as Cb and Ccas. These capacitances shunt the biasing noise to ground.
- The biasing affects also the linearity of the inductively-degenerated LNA. The IIP3 depends on the output impedance of the bias circuitry (Zb1). This impedance should be kept small, relative to $r_\pi$ in order to increase the linearity of the transconductance stage. However, the output impedance is typically designed for having a high resistance in order to reduce the

noise contribution of the bias circuitry and to avoid a significant loading of the RF input port.

## 5.2.7 MIXER INTERFACE

The mixers used in current wireless receivers are typically based on Gilbert cell-type mixers, which provide gain and have enough linearity for wireless applications.

The simplified schematic of a Gilbert mixer which can be used in DCRs is shown in **figure 5.10**. The key factor is the configuration of the mixer input transistors.

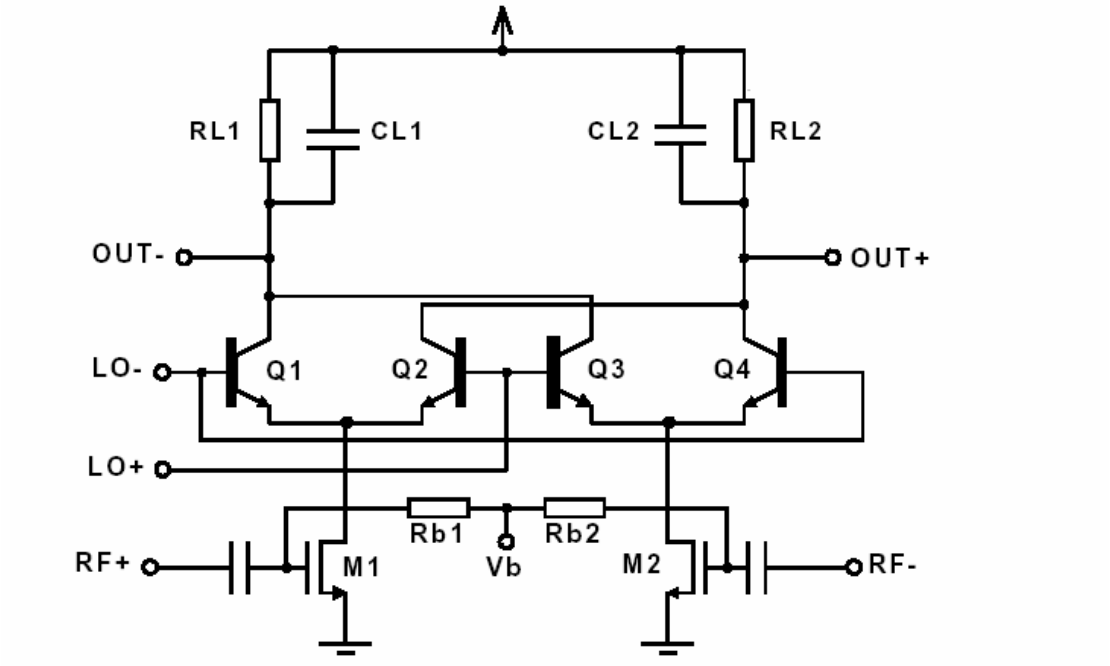


**Figure 5.10** Schematic of a Gilbert cell-type mixer

The mixer is based on two switching pairs, Q1-Q4 and the input transistors M1 and M2. The mixer input signal can be differential or single-ended if the other input is properly AC-grounded. In addition, the input transistor is part of the LNA load. Hence, it has to be taken into account in the simulations. If the LNA uses a resonator load, the mixer input capacitance changes the resonance at low frequencies unless it is properly designed.

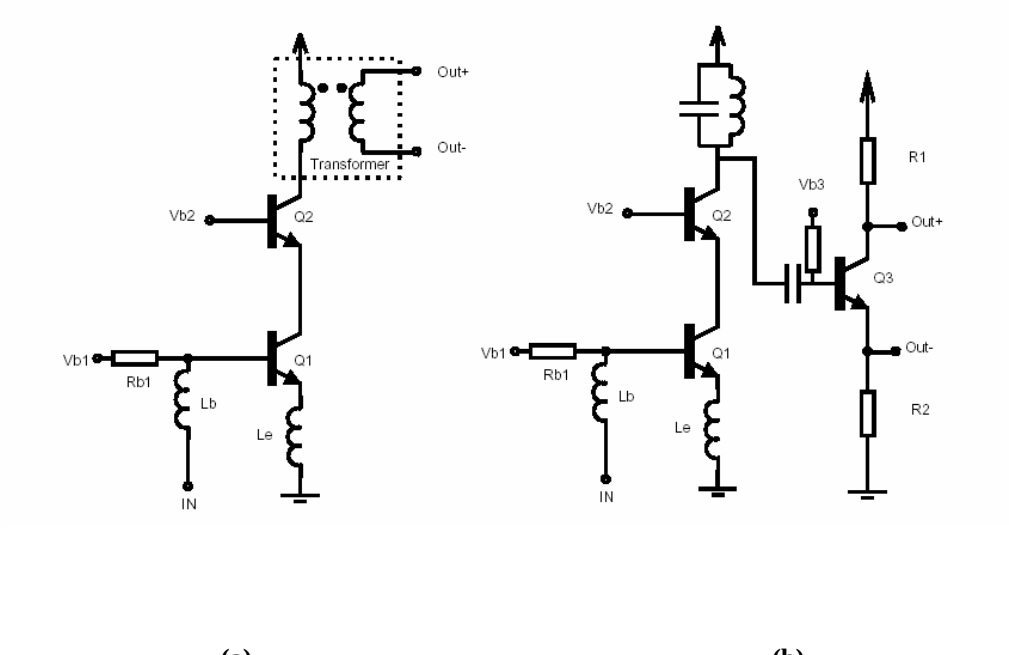


**(a)** **(b)**

**Figure 5.11** Schematic of an inductively-degenerated LNA which has a) a passive and b) an active single-ended-to-differential converter

Depending on the mixer input and the pre-select filter output, a single-ended-to-differential conversion can be required. In this case, the converter can be taken into account in the simulation as a separated block or the LNA-converter combination has to achieve the performance given to the LNA.

Two examples of the conversion implementation can be seen in **figure 5.11**.

## 5.3 VARIABLE GAIN IN INDUCTIVELY-DEGENERATED LNAs

The maximum gain in a LNA is determined by the receiver noise figure and the linearity requirements. The receiver has to be designed in order to receive different signal levels without modifications. The way to achieve this requirement is to establish different gain settings in the receiver. The variable gain can be implemented in the RF circuits and/or in the baseband circuits.

In this chapter, different ways to implement the variable gain in an inductively-degenerated LNA will be explained.

### 5.3.1 ANALOG AND DIGITAL GAIN CONTROL

The variable gain in a RF front-end can be implemented with either analog or digital control.

#### 5.3.1.1 Analog control

The RF front-end can have all the gain values between the maximum and minimum gain settings. The variable gain is adjusted by means of a control voltage or current.

The problem is the non-lineal behavior of the voltage gain as a function of the control current or voltage. The RF gain can be sensitive to the control voltage in certain ranges and less sensitive in others. This leads to a difficult implementation of the engine tuning which controls the LNA gain.

#### 5.3.1.2 Digital control

The RF front-end can only be programmed to several discrete gain settings. The variable gain is adjusted by means of a control code.

If the required number of gain levels increases, the digital control complexity increases as well. In addition, it can produce transients to the receiver output, corrupting then the reception. The gain step may not be constant, leading to big gain changes which can not be managed in the analog baseband or in the A/D converters.

### 5.3.2 GAIN CONTROL IN AN INDUCTIVELY-DEGENERATED LNA

#### 5.3.2.1 Variable gain by using input stage adjustment and load adjustment

According to equations of section 5.2, the LNA voltage gain depends on the load impedance and $G_m$ of the input stage. The LNA gain can be altered if any of these parameters is adjustable. The variable gain implementation in the load or input stage of an inductively-degenerated LNA is shown in **figure 5.12**.

- INPUT STAGE ADJUSTMENT

From equation 5.19, the transconductance of an inductively-degenerated LNA is:

$$G_m = \frac{1}{\omega_r L_e}$$

Since $G_m$ and the input matching are related to each other, the adjustment of a single parameter affects both parameters. In order to a variable gain and a constant input matching, $g_m$ and the inductors Lb1 and Le1 must be adjusted. This leads to a too complicated adjustment and the noise figure increases as a result of the switched adjustable inductors.

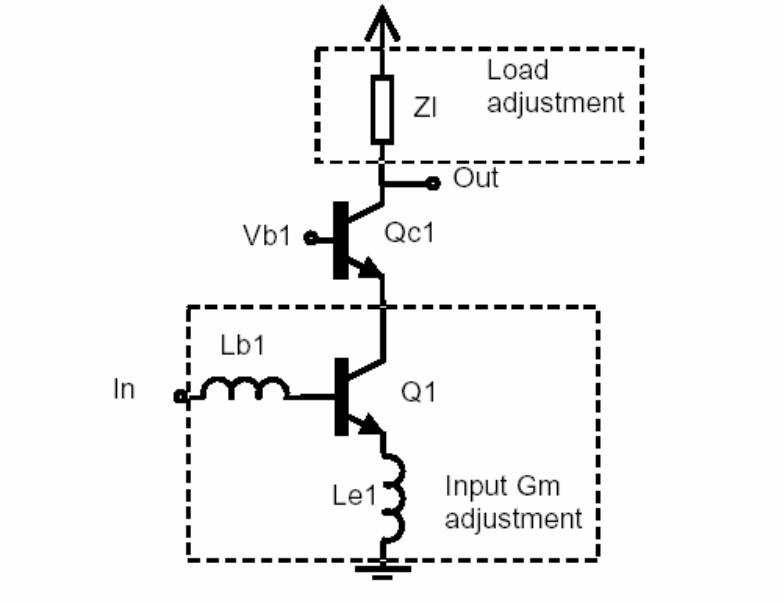


**Figure 5.12** Gain adjustment by changing the load or input $G_m$ of an inductively-degenerated LNA

- LOAD ADJUSTMENT

In can be implemented in different ways and depends on the load type chosen for the LNA.

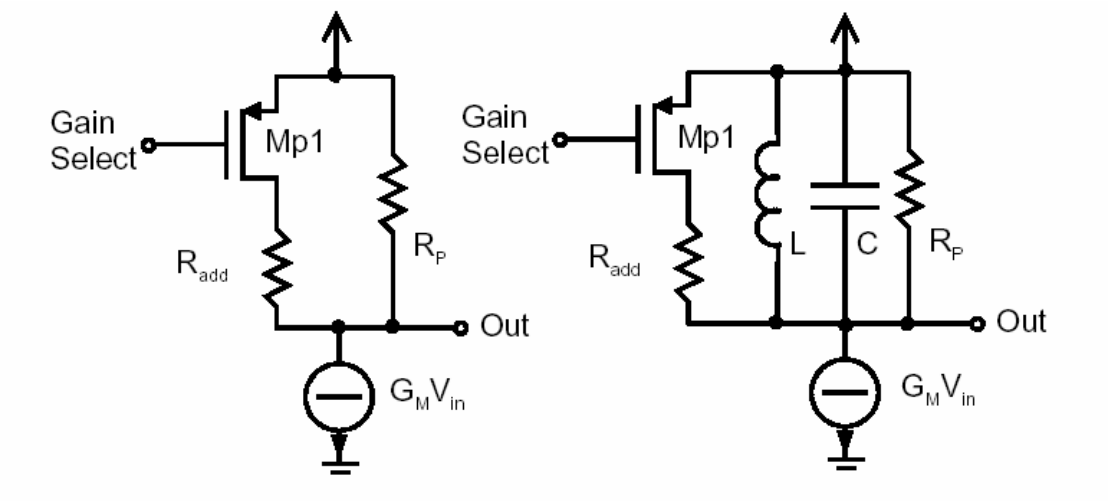


(a) (b)

**Figure 5.13** Gain adjustment of a) a resistive-load LNA and b) a resonator-load LNA

**a) Gain adjustment of a LNA with resistive load**

The resistive load impedance can be adjusted by connecting an additional resistor, $R_{add}$, in parallel with the nominal resistor, $R_{P,}$ with the switch Mp1.

The problem of this implementation is the additional capacitance at the LNA output. When the number of the gain steps increases, the parasitic capacitance resulting from the additional switches and resistors increases and limit the available operation frequencies, which also affects the gain step at high frequencies.

**b) Gain adjustment of a LNA with resonator load**

According to equation 5.28, the impedance at the resonance frequency is:

$$Z(f_r) = \frac{1}{\frac{1}{R_{add}} + \frac{R_L}{R_L^2 + \omega_r^2 L^2}} \qquad \textbf{(5.34)}$$

If $R_{add}$ is connected in parallel with the resonator, the gain decreases. This approach has two aspects which must be taken into account in the design phase:

1._ The inductor and parallel resistor determine the impedance value when the LNA has a maximum gain. However, at lower gain settings, the resistance has a larger effect on the resonator impedance compared to the inductor. When the process variations are taken into account, the gain step is not kept constant as the inductor and resistor values depend on the different parameters of the process.

2._ The variation of the gain step as a function of the frequency. The equation 5.34 determines the gain step at the resonance frequency. However, this step is not constant as a result of the frequency dependence of the resonator impedance, given in equation 5.26.

$$Z_r(j\omega) = \frac{1}{\frac{1}{R_P} + \frac{R_L}{R_L^2 + \omega^2 L^2} + j\left(\omega C - \frac{\omega L}{R_L^2 + \omega^2 L^2}\right)}$$

Hence, if the resistor, $R_{add}$, is changed, the Q value of the resonator changes. The maximum gain step at the resonance frequency and the step value reduce to zero when the operating frequency is moved away from the resonance.

#### 5.3.2.2 Variable gain implemented by using analog or digital current steering

A LNA using an analog current steering for variable gain is shown in **figure 5.14**.

Qc1 is a regular cascode and Qc2 determines the amount of signal flowing to the load and the supply respectively. The voltage gain of the inductively-degenerated LNA is a function of the voltage difference (V_ctrl – Vb1). The voltage gain starts to decrease when V_ctrl reaches Vb1. The minimum achievable gain depends on the isolation to the output from the different signal nodes.

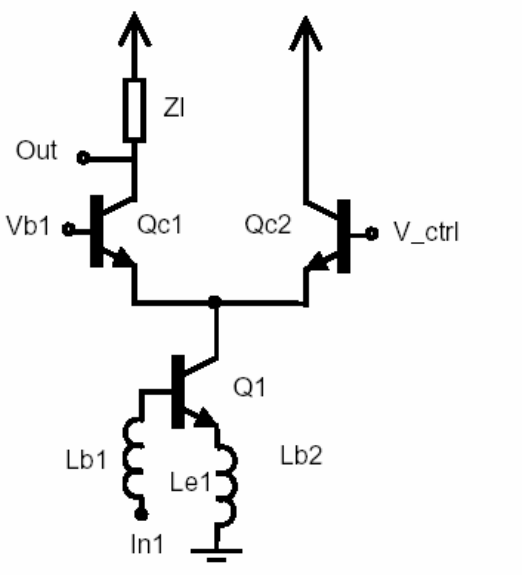


**Figure 5.14** LNA using an analog current steering for variable gain

**Figure 5.15** shows a LNA using a digital current steering for variable gain.

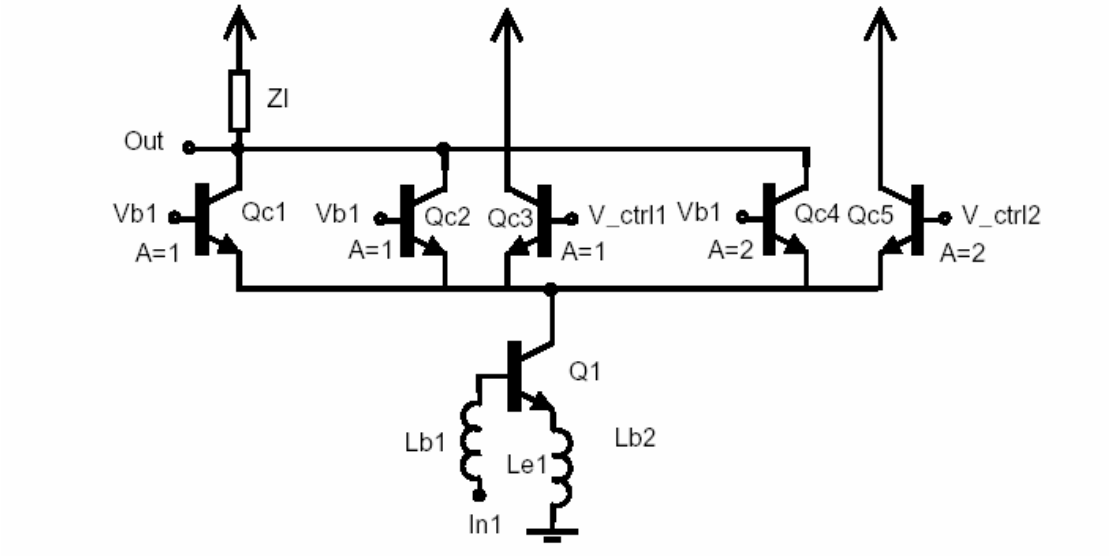


**Figure 5.15** LNA using a digital current steering for variable gain

The gain adjustment is implemented by using additional cascode transistor pairs in parallel with the cascode transistor Qc1. One of the collectors in each pair is connected to the signal output and the other one is the connected to the positive supply. If the bases of Qc2 and Qc4 are to the same bias voltage than Qc1 and the base voltage of Qc3 and Qc5 is equal to ground, the LNA has maximum gain. If the base voltages of one pair are reversed, the voltage gain decreases as:

$$\Delta G = \frac{A_{out}}{A_{out} + A_{VDD}} \qquad \textbf{(5.35)}$$

where:

- $Aout$ is the number of cascode transistors which drive signals to the output.
- $A_{VDD}$ is the number of cascode devices which drive to the positive supply voltage.

Equation 5.35 assumes that all the cascode devices are similar and biased in the way showed above.

#### 5.3.2.3 Variable gain implemented by using resistor chain

The schematic of a LNA which uses a resistor chain for variable gain can be seen in **figure 5.16**.

This implementation is based on digital current steering and load tuning. The gain control is based on the ratio of the resistor values in the resistor row (R1-R3). At maximum gain, the cascode Qc1 drives the signal to the load, which is a damped parallel resonator. The LNA gain is reduced by biasing Qc1 off and having Qc2 or Qc3 on. The gain reduction depends on the R1, R2 and R3 ratio.

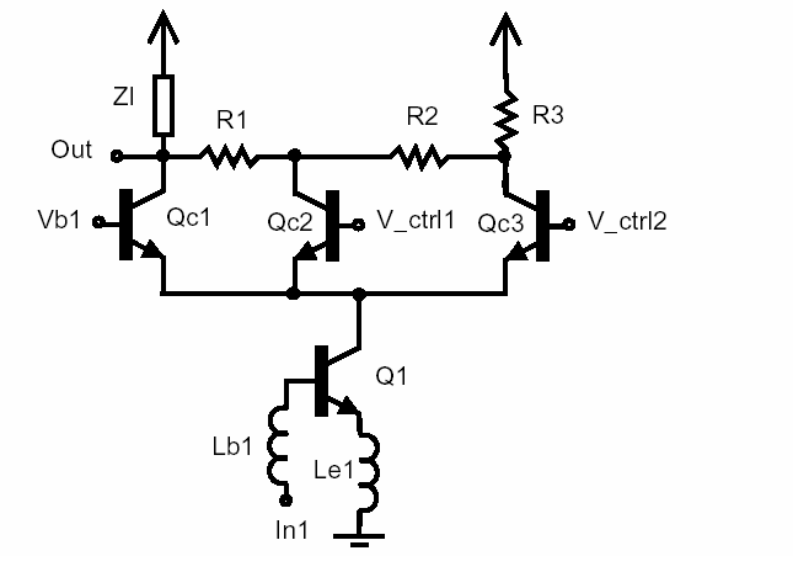


**Figure 5.16** LNA using a resistor chain for variable gain

The benefit of this method is that the gain reduction depends on the ratios between the resistors. Therefore, the process variations do not alter the gain step.

However, this implementation has some disadvantages. The gain control is sensitive to the parasitic capacitances in the resistor chain. In addition, when the gain is reduced, the DC current must go through the resistors in the chain which decreases the DC voltage in the collectors of Qc2 and Qc3.

#### 5.3.2.4 Variable gain implemented by using separated signal paths

An alternative signal path can be used for different gain settings. For a signal closed to the sensitivity level, the inductively-degenerated LNA is biased on when the other stage is biased off. When the signal level at the receiver input increases over a certain threshold level, the alternative path is biased on and the inductively-degenerated stage is turned off.

The schematic of a LNA with an alternative signal path for low-gain mode and an example of the alternative path scheme are shown in **figures 5.17** and **5.18** respectively.

In order to a suitable performance, the additional signal path must have high input impedance when the inductively-degenerated LNA is used. When using the additional signal path, the input matching must fulfill the same performance requirement as in the node of maximum gain. Otherwise, the pre-select filter performance may be degraded and the reception can be then corrupted.

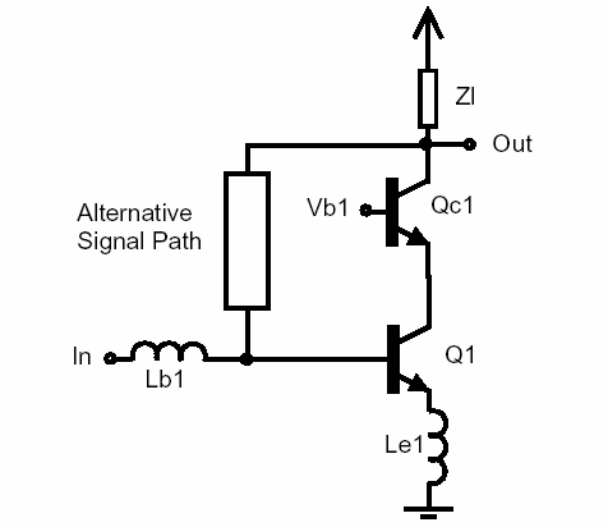


**Figure 5.17** LNA with an alternative signal path for low-gain mode

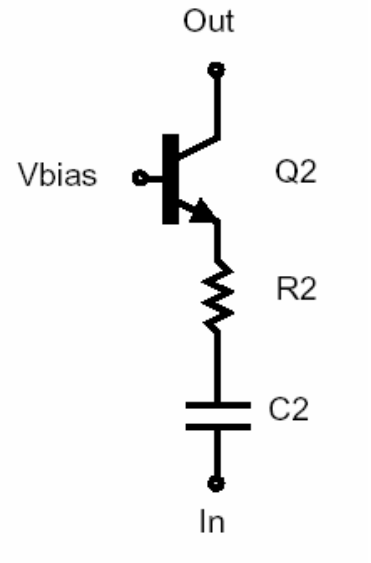


**Figure 5.18** An example of the schematic of the alternative path

The LNA input impedance which has the alternative signal path biased on and the inductively-degenerated LNA biased off is:

$$Z_{in} = j\omega L_{b1} + Z_2 // \left( \frac{1}{j\omega C_\pi} + j\omega L_{e1} \right) \qquad \textbf{(5.36)}$$

where:

- $C_\pi$ is the Q1 base-emitter capacitor.
- $Z_2$ is the input impedance of the additional stage.

$$Z_2 = R_2 + \frac{1}{g_{m2}} + \frac{1}{j\omega C_2} \qquad \textbf{(5.37)}$$

where:

- $g_{m2}$ is the transconductance of Q2.

The implementation of a multi-stage gain control by using separated signal paths is difficult as a change is $g_{m2}$ or R2 also changes the input matching. In addition, the use of multiple parallel stages increases the parasitic components at the LNA input, which always degrades the inductively-degenerated LNA performance. The number of gain steps can be incremented by connecting the alternative signal path between the base and collector of Q1 and by using digital current steering in cascode transistor.

# CHAPTER VI

# RF FRONT-END FOR W-CDMA AND GSM APPLICATIONS

As third generation wireless systems are launched, the coexistence of second- and third-generation cellular systems requires multimode, multiband mobile terminals. The RF front-end presented in this chapter is targeted at GSM and W-CDMA applications and uses the direct-conversion architecture, which is suitable for a high integration level. Its block diagram is shown in **figure 6.1**. It has two separate single-ended input, one input for each standard. With the exception of the input transistors and matching inductors of the LNA, all on-chip devices are utilized in both modes. The single-ended-to-differential conversion is performed before the signal downconversion, thus enabling a double-balanced mixer topology. The RF front-end requires a single LO port because one mode is selected to be operational at a time. The LO is external and a 90° phase shift is performed off-chip.

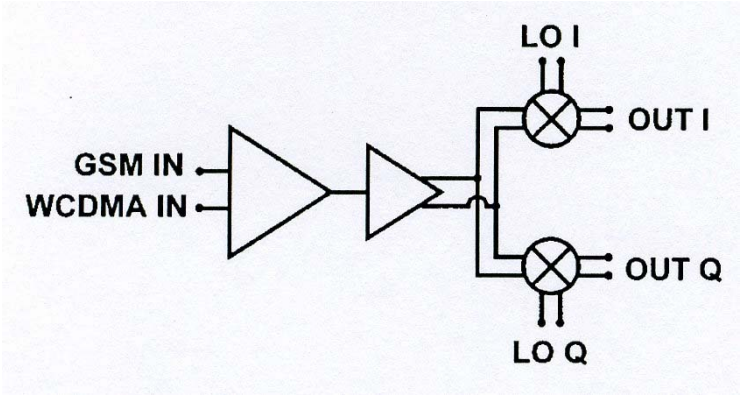


**Figure 6.1** Block diagram of the RF front-end

The RF front-end has been designed for dual-band dual-mode operation. The front-end consumes 22.5mW from a 1.8-V supply and is designed to be used in a direct-conversion W-CDMA and GSM receiver. The front-end has a 27-dB gain control range, which is divided between the LNA and quadrature mixers.

# 6.1 LNA DESIGN

The LNA uses the conventional common-emitter topology with cascode transistors in all gain and mode settings to achieve a good reverse isolation with high gain and mode settings to achieve a good reverse isolation with high gain and low NF. The schematic of the LNA operating in W-CDMA mode with maximum gain is shown in **figure 6.2**.

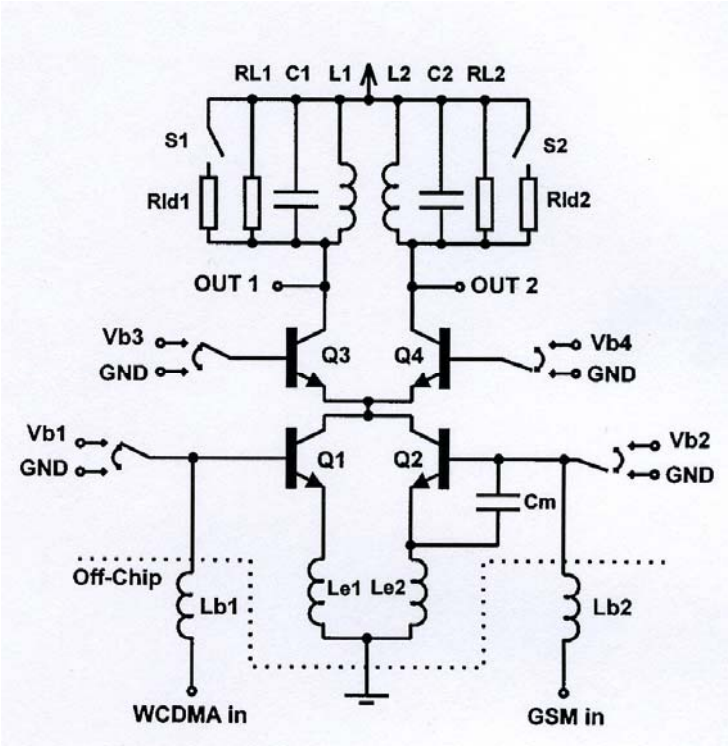


**Figure 6.2** Schematics of the LNA

Transistors Q1 and Q2 are used as the input transistors for different modes. The base and emitter inductors of Q1 and Q2 are used for matching. In the GSM mode, the capacitor Cm is also added between the base and emitter of Q2 to

reduce the value of base inductor Lb2 to a realizable value. Depending whether the LNA is used in W-CDMA or in GSM mode, either of the input transistors is biased on while the other is off. The transistor, which is turned off has a negligible effect on the NF and the signals coming to the base of this transistor are shunted to chip ground. Therefore, the signals laying at the reception band of another standard and thus passing the pre-select filter can not desensitize the LNA.

The LNA has two damped resonators, which are used as load in different modes. The resonance frequencies are 950 MHz and 2.1 GHz, respectively. The damping resistors RL1 (250 Ω) and RL2 (150 Ω) give a sufficient bandwidth for both mobile terminal and base station usage and tolerance against the different process variations without deteriorating the noise performance of the LNA. The -1-dB bandwidths are 350 and 150 MHz for W-CDMA and GSM resonator, respectively. The active output port and the load resonator of the LNA are selected with the biasing of the cascode transistors.

The LNA has two gain steps in both modes, which are implemented in the following manner. In the maximum gain, the LNA uses the damped resonator of the appropriate mode as a load. For example, in W-CDMA mode, the Q1 acts as an input transistor, Q3 as a cascode, and RL1, C1, L1 as load. Depending on the chosen standard, the first gain step is realized by connecting another resistor in parallel with the resonator by closing the PMOS switch S1 or S2 to reduce the Q-value of the resonator. The sizing of the switch constitutes a tradeoff between on-resistance and parasitic capacitance, which both affect damping and resonant frequencies. The gain step is 3.2 dB in GSM mode and 2.8 dB in W-CDMA mode at the resonant frequency, respectively. A larger gain step in the LNA is performed connecting the resonator tuned for the other mode as a load. In that

case, LNA does not operate at the resonance frequency and the gain is lowered over 12 dB compared to the maximum. For example, in W-CDMA mode, this gain step is performed by connecting Q3 to chip ground and using Q4 as a cascode. In that case, the LNA uses resonator L2, C2 and RL2 as load and OUT2 instead of OUT1. The gain and mode control in the LNA is implemented using MOs switches, which steer the biasing of Q1-Q4 turning off the biasing of the unused devices. The input transistors are biased using current mirrors while the cascade transistors use $V_{be}$ multipliers. The LNA drives an ac-coupled single-ended-to-differential converter.

## 6.2 SINGLE-ENDED-TO-DIFFERENTIAL CONVERTER

The single-ended-to-differential converter enables the use of double-balanced mixers and isolates the LNA load resonators. The schematic is shown is **figure 6.3**. The conversion is performed with the either transistor Q5 or Q6 depending on the chosen LNA resonator. This kind of structure has some benefits compared to passive baluns or differential pair converters. The integrated passive baluns are not feasible because they require a large area and can not be used in the whole frequency band from 900 MHz to 2.2 GHz. The differential pair on the other hand can not fulfill the high linearity requirements with a low supply and low current.

The converter has a 3-dB voltage gain when connected to the front-end. The maximum voltage gain to a high impedance load is 6 dB for this type of a converter. In order to achieve a good balance, the load impedances seen from the emitter and collector of Q5 and Q6 must match well. Therefore, the supply inductances L1 and L2 should also be equal. This was solved by using separate supply pads in the converter to ensure the equal lengths and number of bond

wires. According to the simulations, the phase and gain errors are less than 4° and 0.2 dB over the operation range from 800 MHz to 2.2 GHz, respectively. The single-ended LNA and the single-ended-to differential converter are sensitive to supply noise. Therefore, an on-chip decoupling 100-pF capacitor with a small series resistor provides efficient damping without susceptibility to unwanted resonances.

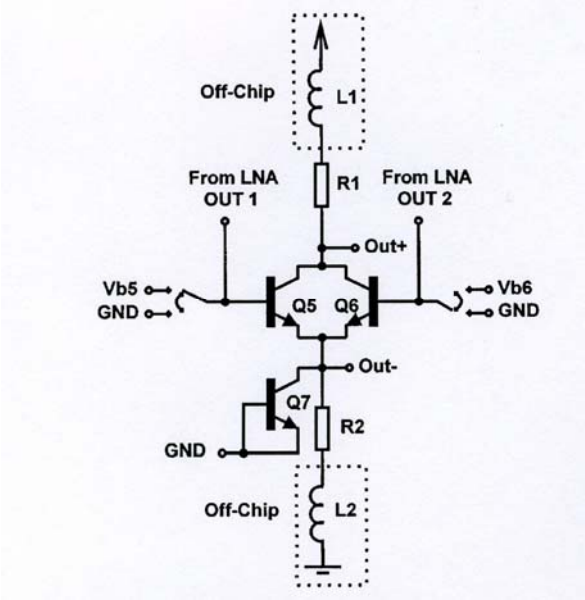


**Figure 6.3** Schematic of the single-ended to differential converter

## 6.3 MIXER DESIGN

The mixer is basically a double-balanced cross-coupled Gilbert mixer. Its schematic is shown in **figure 6.4**. It utilizes NMOS transistors in its input stage with bipolar LO-switches. The advance of using MOS transconductors (M1-M2), rather than bipolars, is in the better linearity performance. In addition, the mixer

topology is current boosted to better relax the lower supply voltage conditions. The boosting enables the utilization of higher mixer conversion gain by allowing the larger resistive loading in the mixer output. By current boosting, a lower mixer noise figure is achieved without deteriorating the third-order linearity performance. In this type of mixer without current boosting, the linearity and noise performance always trade off each other. The linearity of the input transconductors can be maintained since the drain currents through the devices do not need to be lowered. The additional dc currents, $I_1$-$I_2$, are fed through resistively degenerated long-channel PMOS transistors.

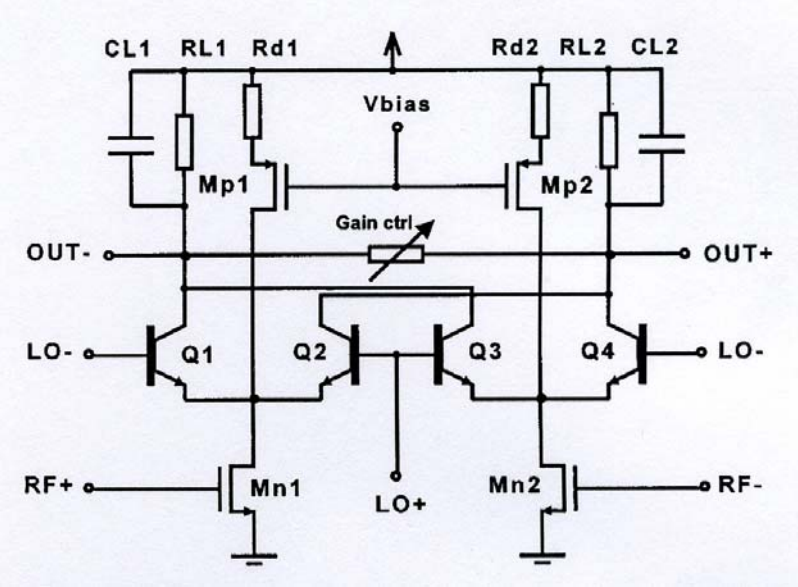


**Figure 6.4** Schematic of the mixer

The bipolar switching transistors (Q1-Q4) are used as the functional mixer core instead of the respective NMOS transistors due to their lower flicker noise. In addition, the bipolars provide a higher $f_T$, which is required in order to achieve as symmetrical on-off switching as possible. Thus, the second-order distortion

caused by the nonideal LO signal duty cycle is minimized. In addition, MOS switches typically require a larger swing to exhibit complete switching compared to bipolars. This relaxes the LO cross coupling and isolation performance. The mixers provide adjustable voltage conversion gain with three 4-dB gain control steps. The maximum voltage conversion gain is 14 dB. The gain control is implemented by switching additional resistors pairs between the mixer output terminals. The mixer has a RC lowpass pole at the output to relax the out-of-band linearity requirements of the following baseband stages.

## 6.4 EXPERIMENTAL RESULTS

The measured performance of the RF front-end is summarized in **table 6.1**. The RF responses of both modes with the maximum gain settings are shown in **figure 6.5**. The maximum achieved gain in GSM mode was 39 dB while in W-CDMA mode was 33 dB. **Figure 6.6** illustrates all 12 possible gain values that can be achieved in W-CDMA mode and **figure 6.7** shows the RF responses of six different gain settings in GSM mode. Curve A illustrates the maximum gain setting. Curves B-D show the mixer gain steps as the LNA gain is at maximum. Curves E and F present the LNA gain steps while the mixer has minimum gain. Total gain control range is 27 dB for both modes. The variation in the gain, due to the RF response, between the mobile station reception and base station reception bands is less than 1 dB in all settings.

The input matching in **figure 6.8** is independent of the front-end gain because the biasing of the input transistor remains the same with the different gain settings. The reported S11 values for GSM and W-CDMA cover both mobile station and base station reception bands.

| | W-CDMA | GSM |
|---|---|---|
| NF @ max gain [dB] | 4.3 | 2.3 |
| NF @ min gain [dB] | 15.9 | 12.3 |
| Voltage gain max [dB] | 33 | 39.5 |
| Voltage gain min [dB] | 6.5 | 12 |
| IIP3 @ max gain [dBm] | -14.5 | -19 |
| IIP3 @ min gain [dBm] | -7 | -7.5 |
| IIP2 @ max gain [dBm] | +34 | +35 |
| IIP2 @ min gain [dBm] | +32 | +34 |
| ICP -1dB @ max gain [dBm] | -25 | -29 |
| ICP -1 dB @ min gain [dBm] | -20 | -23 |
| LO-to-RF isolation [dB] | >58 | >68 |
| S11 [dB] | <-18 | <-12 |
| P(LO) [dBm] | -10 | -10 |
| Power dissipation [mW] | 22.5 | 21.5 |
| Supply voltage [V] | 1.8 | 1.8 |

**Table 6.1** Measured performance in W-CDMA and GSM modes

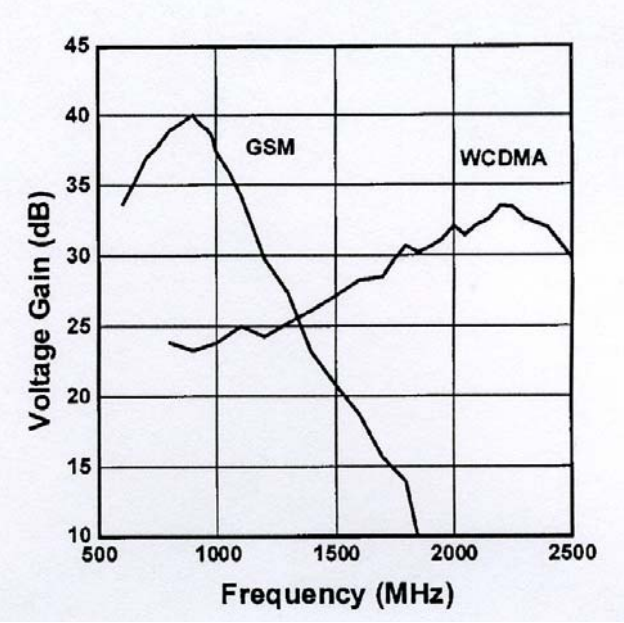


**Figure 6.5** Maximum gain responses on both modes

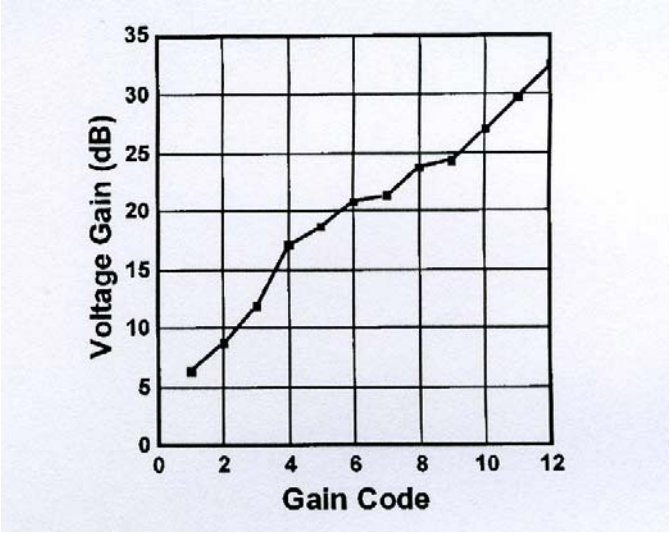


**Figure 6.6** Gain of W-CDMA mode at different tuning codes

**Figure 6.9** illustrates the frequency response of the output noise power with maximum gain in both modes. The noise figures are 2.3 and 4.3 dB for GSM and W-CDMA, respectively. The low-flicker noise corner was achieve with bipolar LO switching transistors and with a sufficient gain in the front-end. The contribution of the flicker noise in the total noise figure is almost negligible even in the GSM. The measured noise figure in the GSM mode when integrated from 200 Hz to 100 KHz increases only by 0.2 dB compared to white noise. In W-CDMA the flicker noise is insignificant.

**Figure 6.10** illustrates the linearity of the front-end in W-CDMA mode in the maximum gain. The effects of the supply voltage to gain, IIP2 and IIP3, are shown in **figure 6.11** and **figure 6.12** for GSM and W-CDMA respectively.

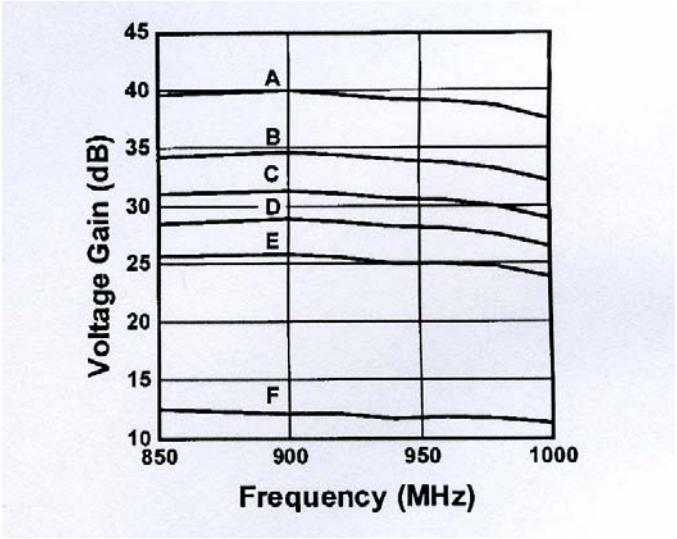


**Figure 6.7** RF response with six different gain settings in the GSM mode

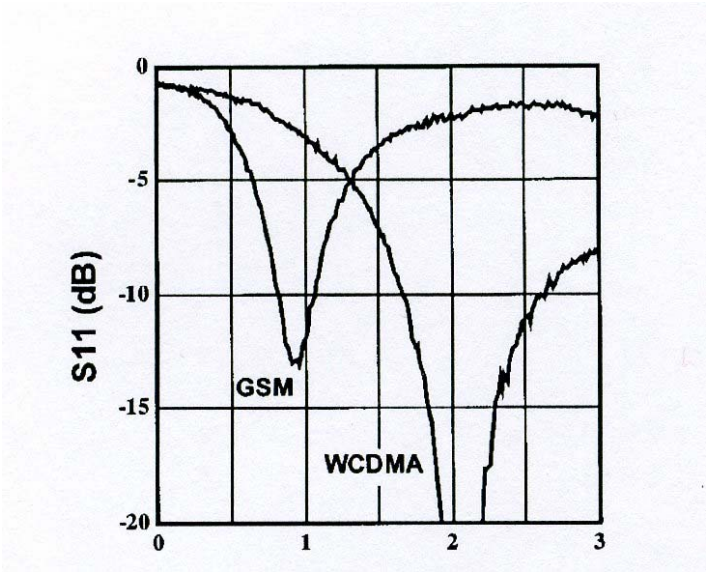


**Figure 6.8** Input matching on both bands

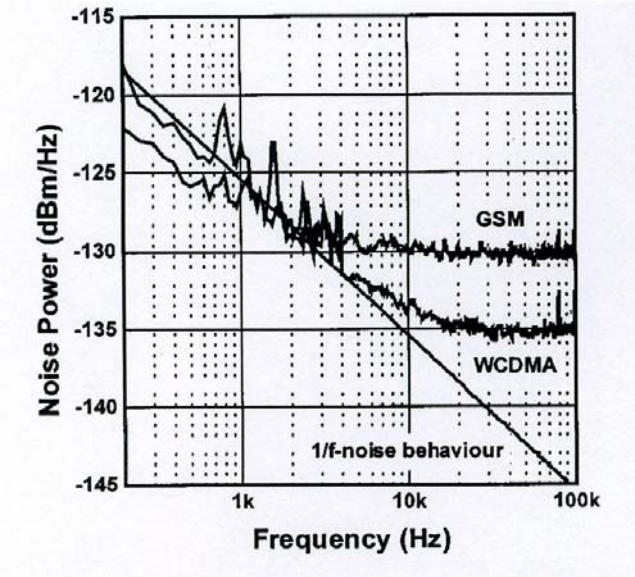


**Figure 6.9** Output noise power in W-CDMA and GSM maximum gain settings

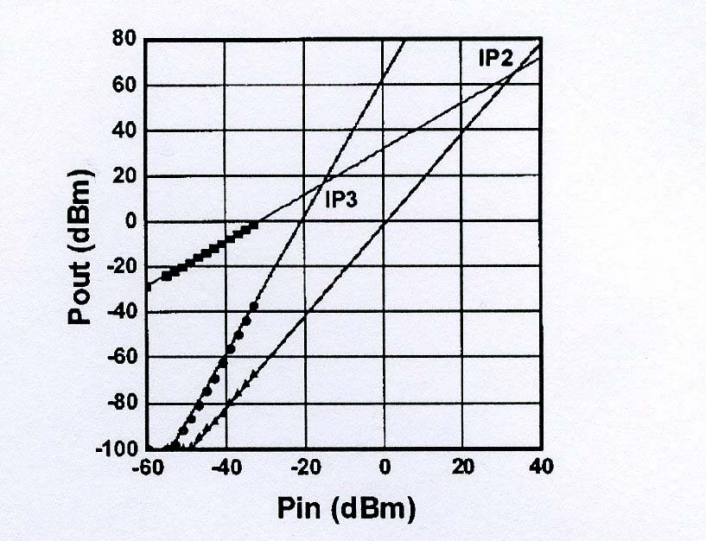


**Figure 6.10** Linearity of RF front-end in W-CDMA maximum gain mode

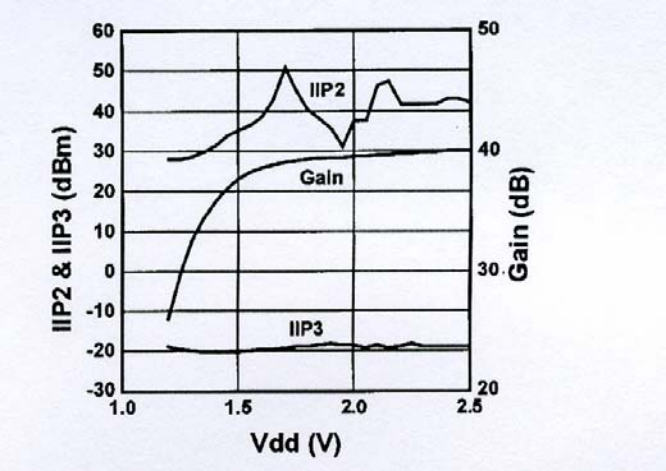


**Figure 6.11** Gain, IIP2 and IIP3 as a function of supply voltage in the GSM mode

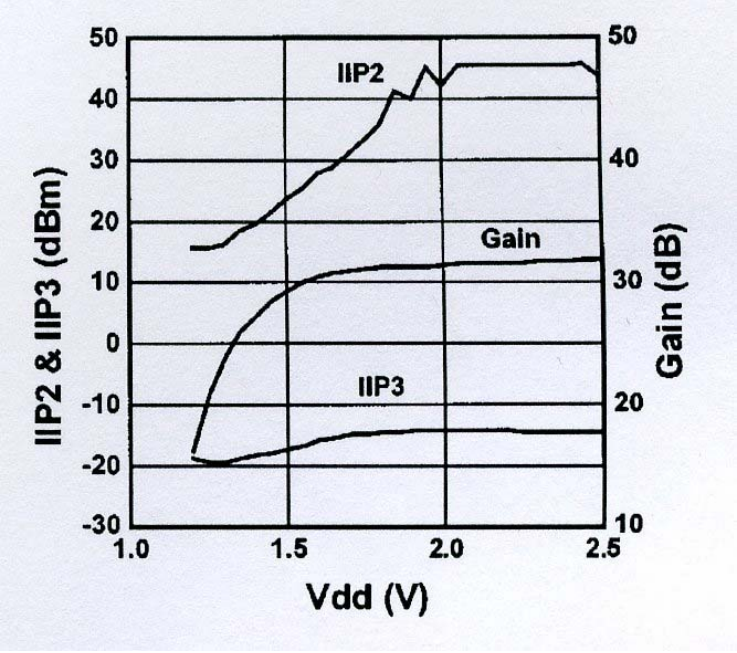


**Figure 6.12** Gain, IIP2 and IIP3 as a function of supply voltage in the W-CDMA mode

# REFERENCES


[1] Rafael Herradón Díez, “Comunicaciones Móviles Digitales”, in Publicaciones E.U.I.T. de Telecomunicación, March 2003.

[2] Rafael Herradón Díez, “Comunicaciones Móviles Digitales II”, in Publicaciones E.U.I.T. de Telecomunicación, March 2003.

[3] Harri Holma, Antti Toskala, “WCDMA for UMTS”, ed. John Wiley & Sons, LTD, second edition, 2002.

[4] J. Ryynänen, K. Kivekäs, J. Jussila, A. Pärssinen, K. Halonen, ”A Dual-Band RF Front-End for WCDMA and GSM applications”, IEEE J. Solid-State Circuits, vol. 36, pp.1198-1204, August 2001.

[5] J. Ryynänen, “Low-Noise Amplifiers for Integrated Multi-Mode Direct Conversion Receivers”, http://lib.tkk.fi/Diss/2004/isbn9512271109/isbn9512271109.pdf, January 2005.

[6] S.K. Reynolds, B.A. Floyd, T.J. Beukema, T. Zwick, U.R. Pfeiffer, H.A. Ainspan, “A direct-conversion receiver integrated circuit for WCDMA mobile systems”, http://www.research.ibm.com/journal/rd/472/reynolds.pdf, February 2005.

[7] http://www.umtsworld.com, January 2005

[8] Hongying Yin, “Radio Receiver Architecture”, http://www.comlab.hut.fi/opetus/333/2004_2005_slides/Receiver_architectures.pdf, March 2005.